Science Advances
AAAS

advances.sciencemag.org/cgi/content/full/4/10/eaau1956/DC1

Supplementary Materials for

Poly(amide-imide) materials for transparent and flexible displays

Sun Dal Kim, Byungyong Lee, Taejoon Byun, Im Sik Chung, Jongmin Park, Isaac Shin, Nam Young Ahn, Myungeun Seo, Yunho Lee, Yeonjoon Kim, Woo Youn Kim, Hyukyun Kwon, Hanul Moon, Seunghyup Yoo, Sang Youl Kim*

*Corresponding author. Email: kimsy@kaist.ac.kr

Published 26 October 2018, *Sci. Adv.* **4**, eaau1956 (2018)
DOI: 10.1126/sciadv.aau1956

This PDF file includes:

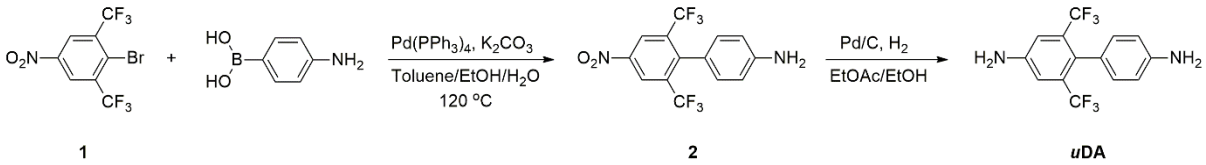

Fig. S1. Synthetic route to *u*DA.

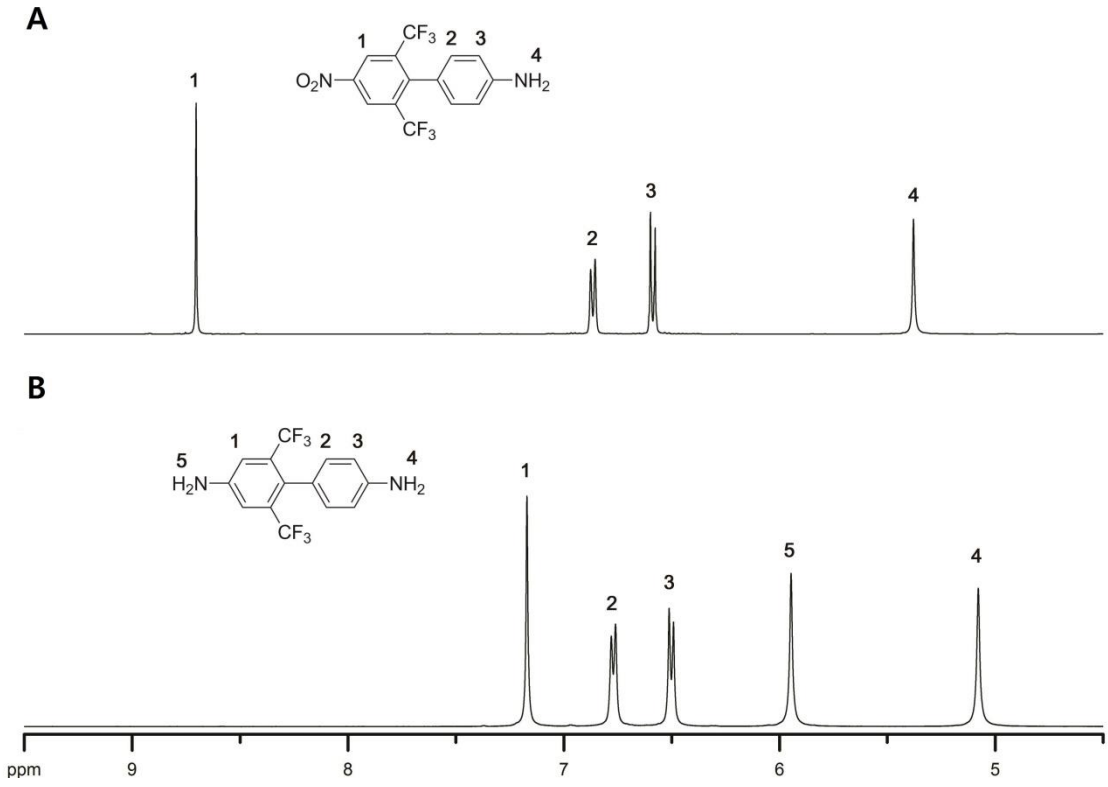

Fig. S2. ^{1}H NMR spectra of (A) the nitro intermediate 2 and (B) *u*DA.

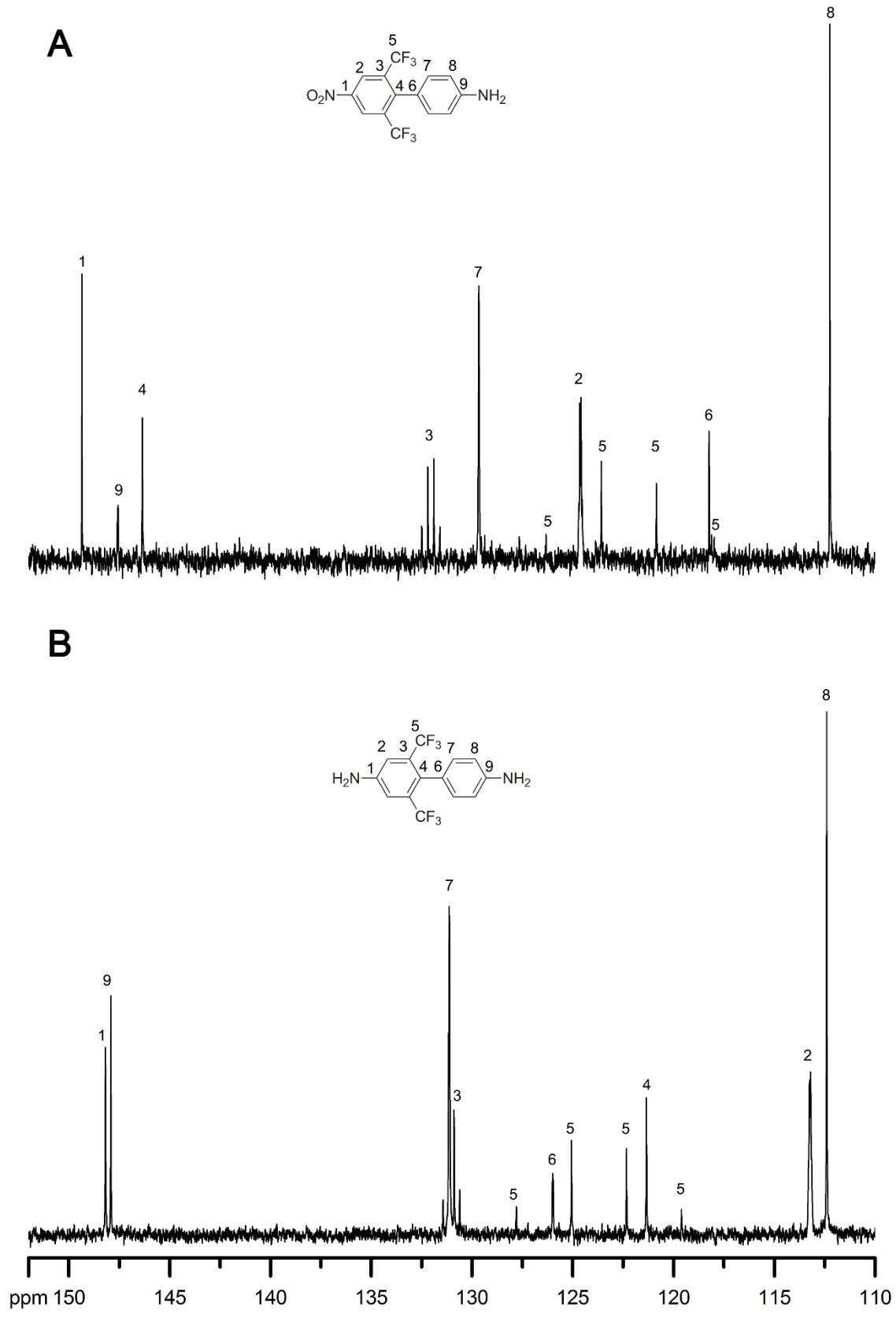

Fig. S3. ^{13}C NMR spectra of (A) the nitro intermediate 2 and (B) *u*DA.

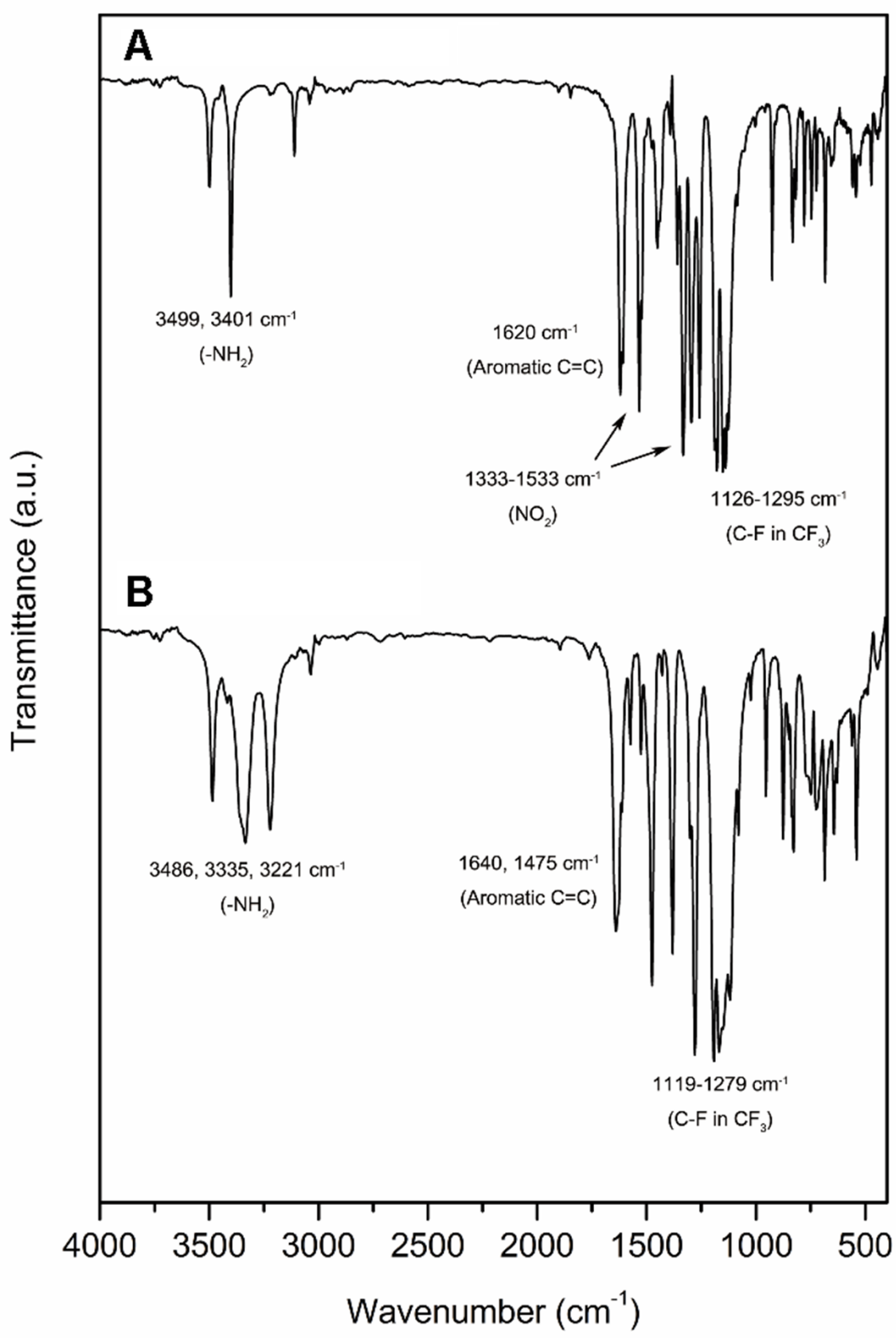

Fig. S4. FTIR spectra of (A) the nitro intermediate 2 and (B) *u*DA.

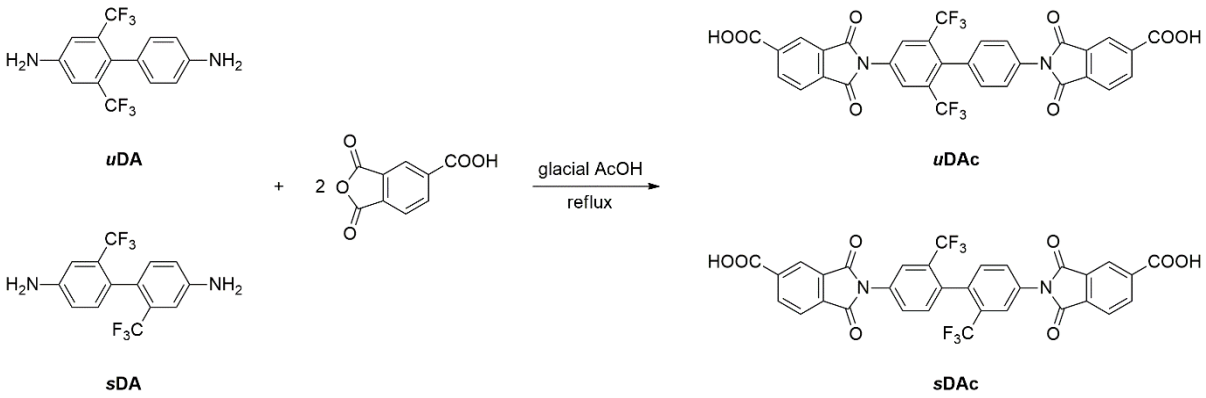

Fig. S5. Synthetic route to diacids.

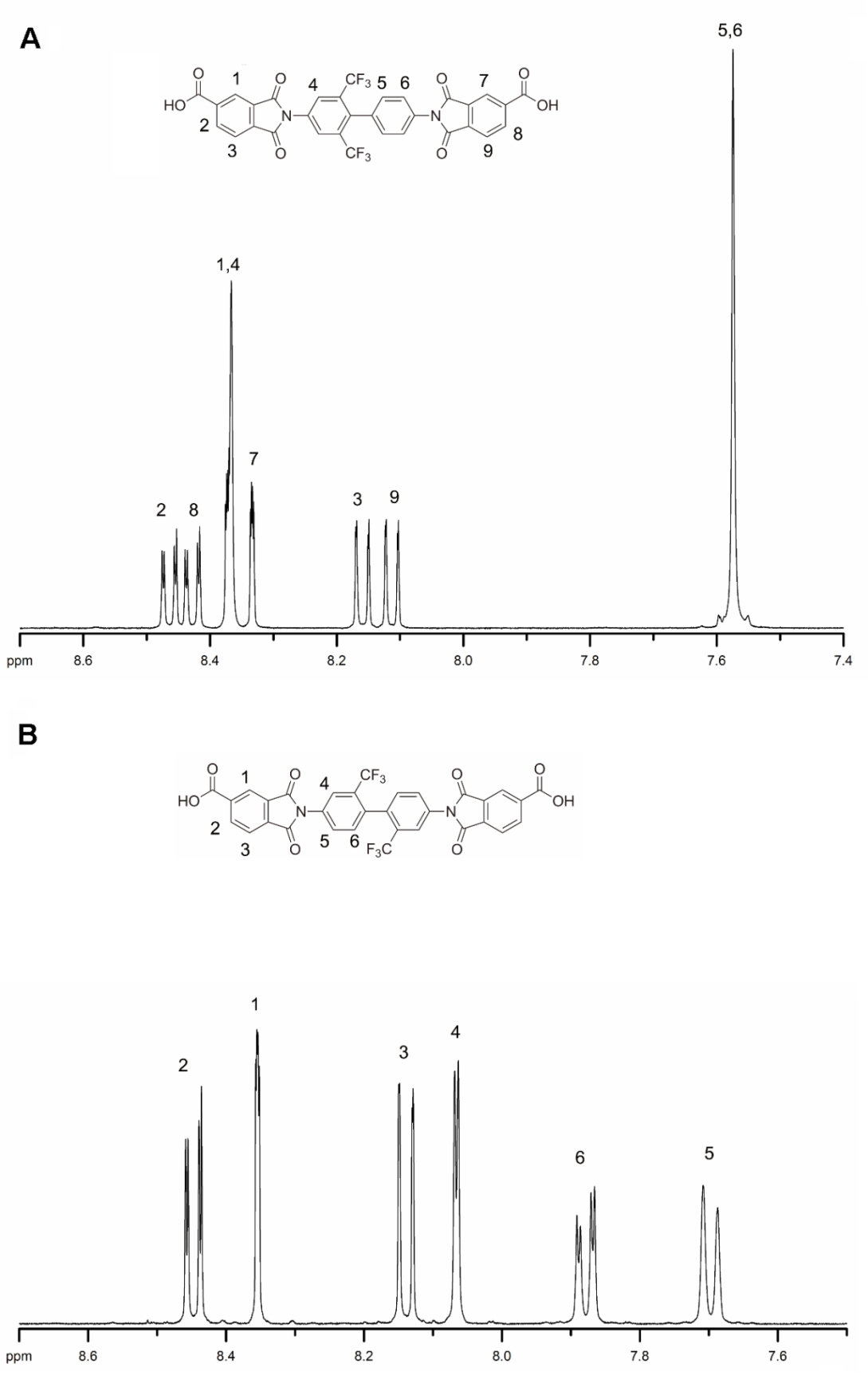

Fig. S6. ^{1}H NMR spectra of the diacids (A: *u*DAc, B: *s*DAc).

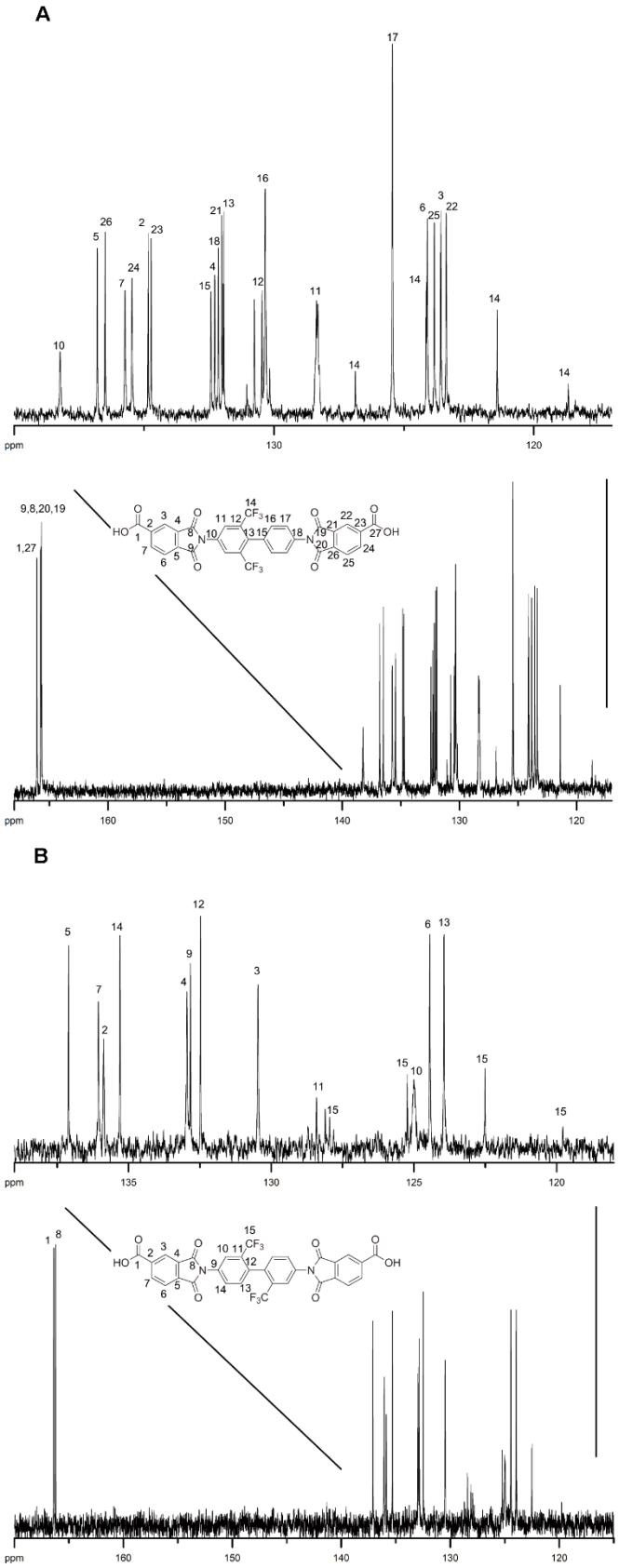

Fig. S7. ^{13}C NMR spectra of the diacids (A: *u*DAc, B: *s*DAc).

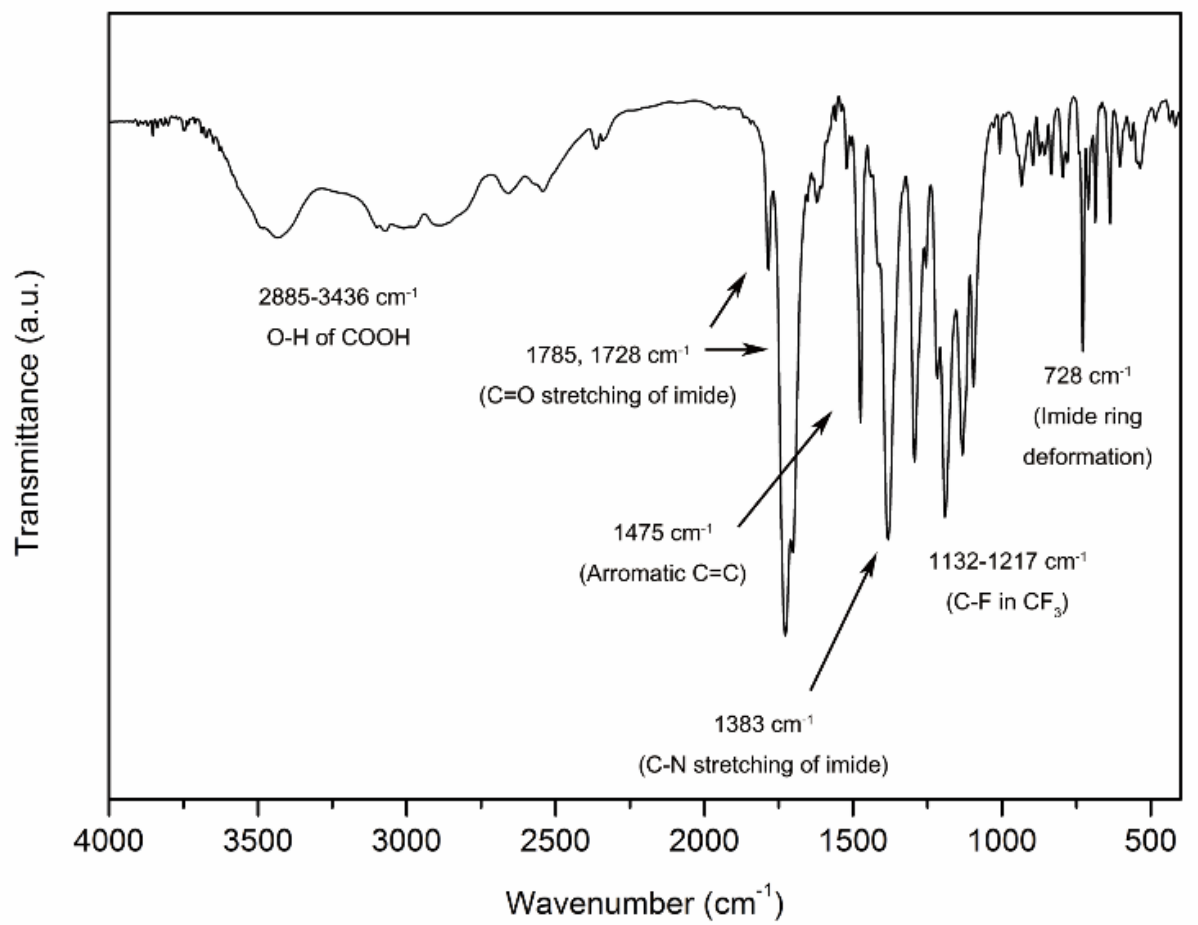

Fig. S8. FTIR spectrum of *u*DAc.

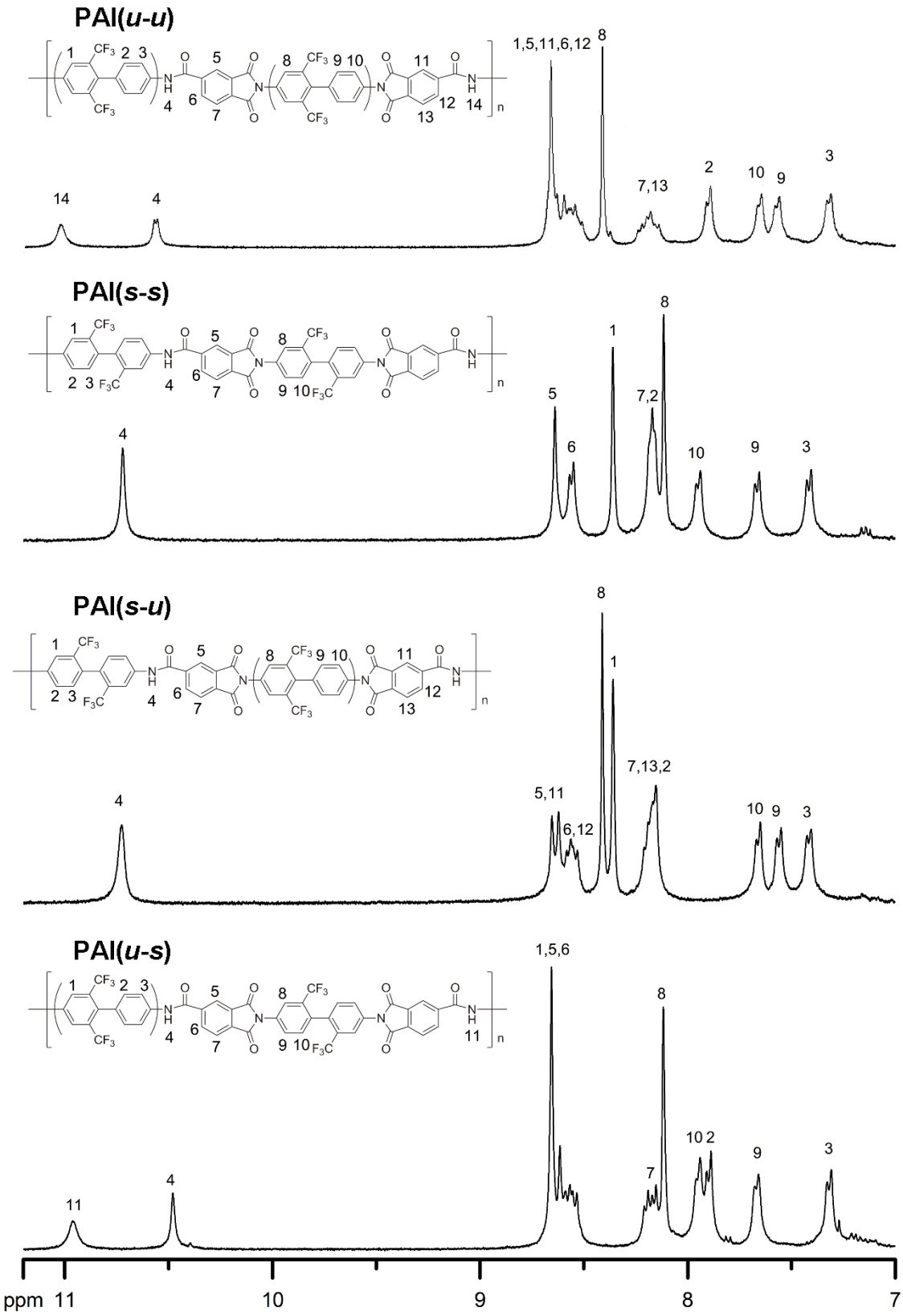
PAI(u-u)
1,5,11,6,12
8
14
4
7,13
2
10
9
3
PAI(s-s)
8
1
5
7,2
6
4
10
9
3
PAI(s-u)
8
1
7,13,2
5,11
6,12
4
10
9
3
PAI(u-s)
1,5,6
8
10 2
9
3
7
4
11
ppm 11
10
9
8
7

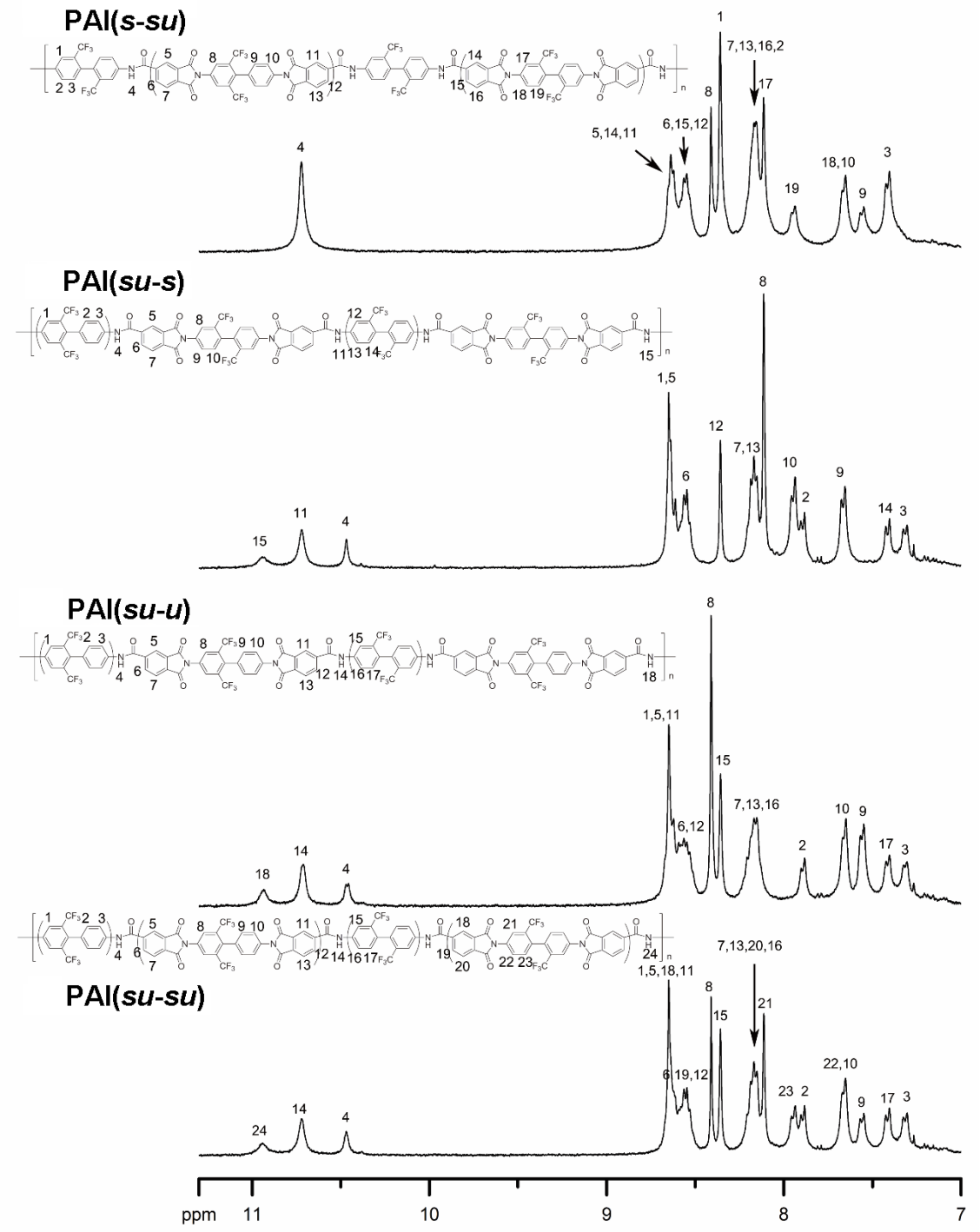

Fig. S9. ^{1}H-NMR spectra of PAIs.

Table S1. Solubility of PAIs.

Solvents	**PAI (*u*-*u*)**	**PAI (*s*-*s*)**	**PAI (*s*-*u*)**	**PAI (*u*-*s*)**	**PAI (s-*su*)**	**PAI (*su*-*s*)**	**PAI (*su*-*u*)**	**PAI (*su*-*su*)**
THF	++	++	++	++	++	++	++	++
DMF	++	++	++	++	++	++	++	++
DMSO	++	++	++	++	++	++	++	++
NMP	++	++	++	++	++	++	++	++
DMAc	++	++	++	++	++	++	++	++
m-Cresol	++	++	++	++	++	++	++	++
Ethyl acetate	-	-	-	-	-	-	-	-
Acetone	-	-	-	-	-	-	-	-
Anisole	-	-	-	-	-	-	-	-
Chloroform	-	-	-	-	-	-	-	-
ODCB	-	-	-	-	-	-	-	-
Acetonitrile	-	-	-	-	-	-	-	-
Toluene	-	-	-	-	-	-	-	-
Diethyl ether	-	-	-	-	-	-	-	-
n-hexane	-	-	-	-	-	-	-	-
methanol	-	-	-	-	-	-	-	-

[a]Solubility: ++, soluble at room temperature; -, insoluble. Abbreviations: THF, tetrahydrofuran; DMF, *N*,*N*-dimethylformamide; DMSO, dimethyl sulfoxide; NMP, *N*-methylpyrrolidone; DMAc, *N*,*N*-dimethylacetamide; ODCB, 1,2-dichlorobenzene.

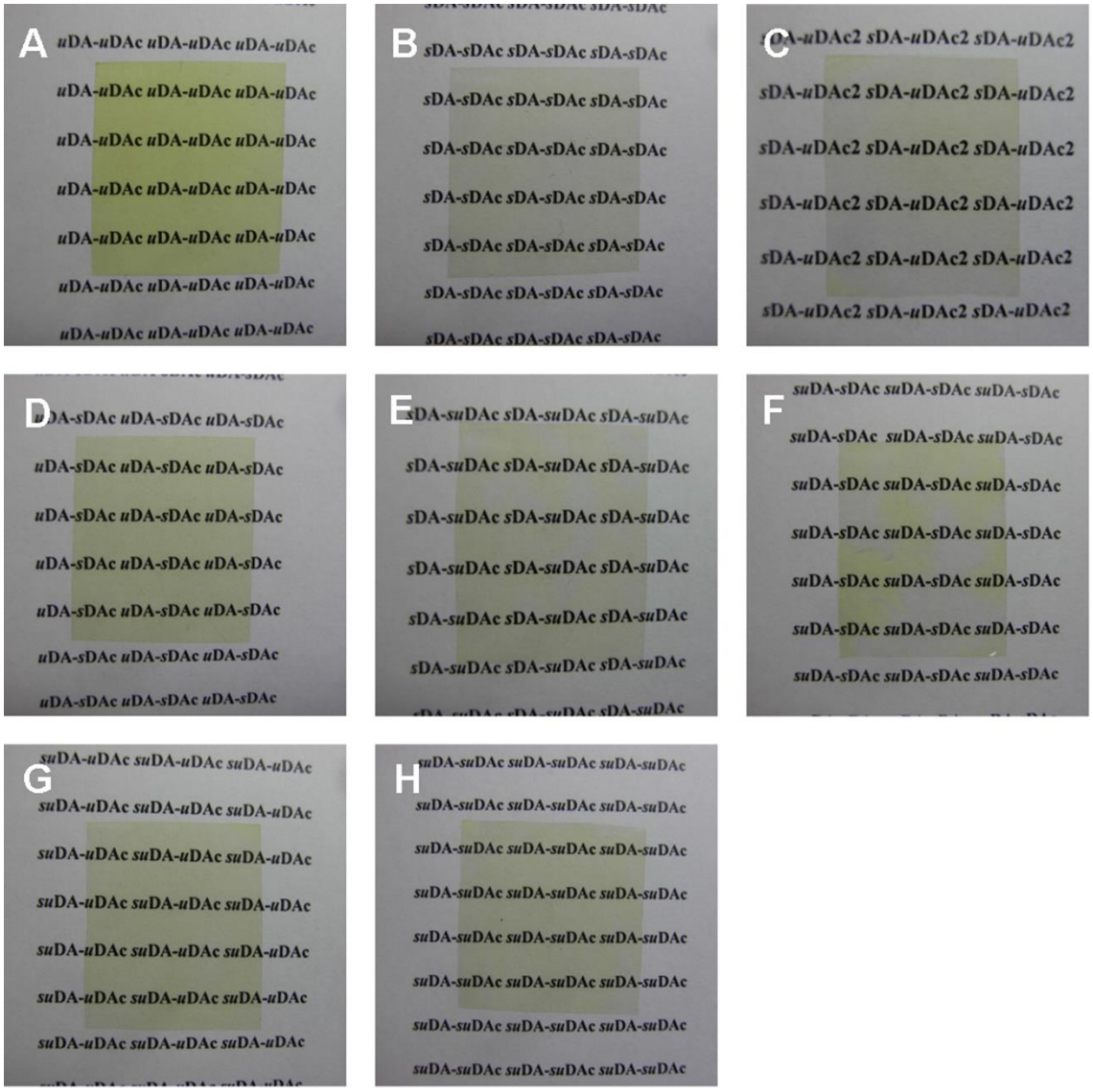

Fig. S10. Photos of PAIs films. (A) **PAI(*u*-*u*)**, (B) **PAI(*s*-*s*)**, (C) **PAI(*s*-*u*)**, (D) **PAI(*u*-*s*)**, (E) **PAI(*s*-*su*)**, (F) **PAI(*su*-*s*)**, (G) **PAI(*su*-*u*)**, (H) **PAI(*su*-*su*)**.

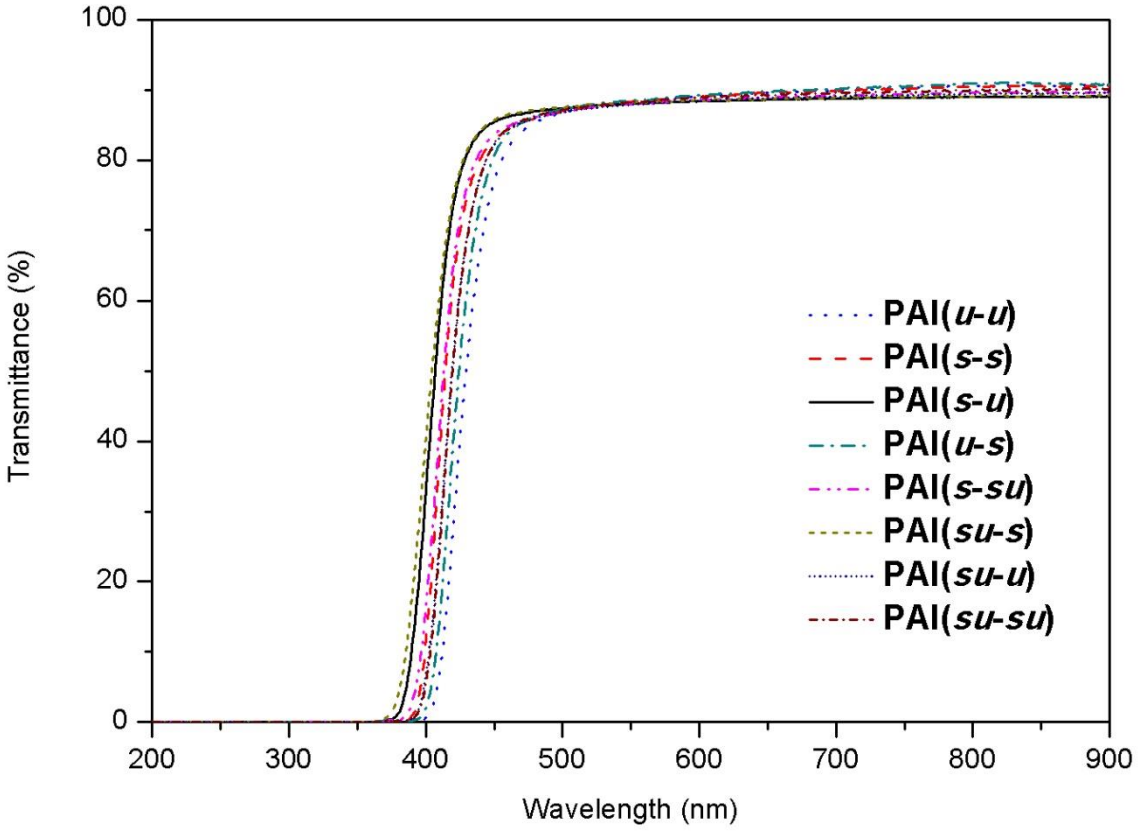

Fig. S11. UV-Visible spectra of PAIs.

Table S2. Birefringence of PAIs.

λ (nm)	Polymer code	n_{TE}[a]	n_{TM}[b]	n_{av}[c]	Δn[d]	ε[e]	d(μm)[f]
633	**PAI(*u*-*u*)**	1.638	1.517	1.598	0.121	2.81	14.8
	PAI(*s*-*s*)	1.648	1.513	1.603	0.135	2.83	6.5
	PAI(*s*-*u*)	1.645	1.506	1.599	0.139	2.81	13.7
	PAI(*u*-*s*)	1.641	1.516	1.599	0.125	2.81	3.0
	PAI(*s*-*su*)	1.647	1.510	1.601	0.137	2.82	8.8
	PAI(*su*-*s*)	1.644	1.518	1.602	0.126	2.82	3.2
	PAI(*su*-*u*)	1.641	1.508	1.597	0.133	2.81	7.1
	PAI(*su*-*su*)	1.642	1.514	1.599	0.128	2.81	8.7
1310	**PAI(*u*-*u*)**	1.604	1.498	1.569	0.106	2.71	14.7
	PAI(*s*-*s*)	1.615	1.495	1.575	0.120	2.73	6.5
	PAI(*s*-*u*)	1.612	1.489	1.571	0.123	2.71	13.6
	PAI(*u*-*s*)	1.608	1.497	1.571	0.111	2.71	3.1
	PAI(*s*-*su*)	1.610	1.491	1.570	0.119	2.71	8.5
	PAI(*su*-*s*)	1.610	1.499	1.573	0.111	2.72	3.3
	PAI(*su*-*u*)	1.606	1.492	1.568	0.114	2.70	7.3
	PAI(*su*-*su*)	1.607	1.494	1.569	0.113	2.71	9.4

[a]n_{TE}: the in-plane refractive index. [b]n_{TM}: the out-of-plane refractive index. [c]n_{av}: the average refractive index ($n_{av} = (2n_{TE} + n_{TM})/3$). [d]$\Delta n$: birefringence ($n_{TE} - n_{TM}$). [e]Dielectric constant estimated from the refractive index: $\varepsilon \approx 1.10 n_{av}^2$ [f]Film thickness for the refractive index measured.

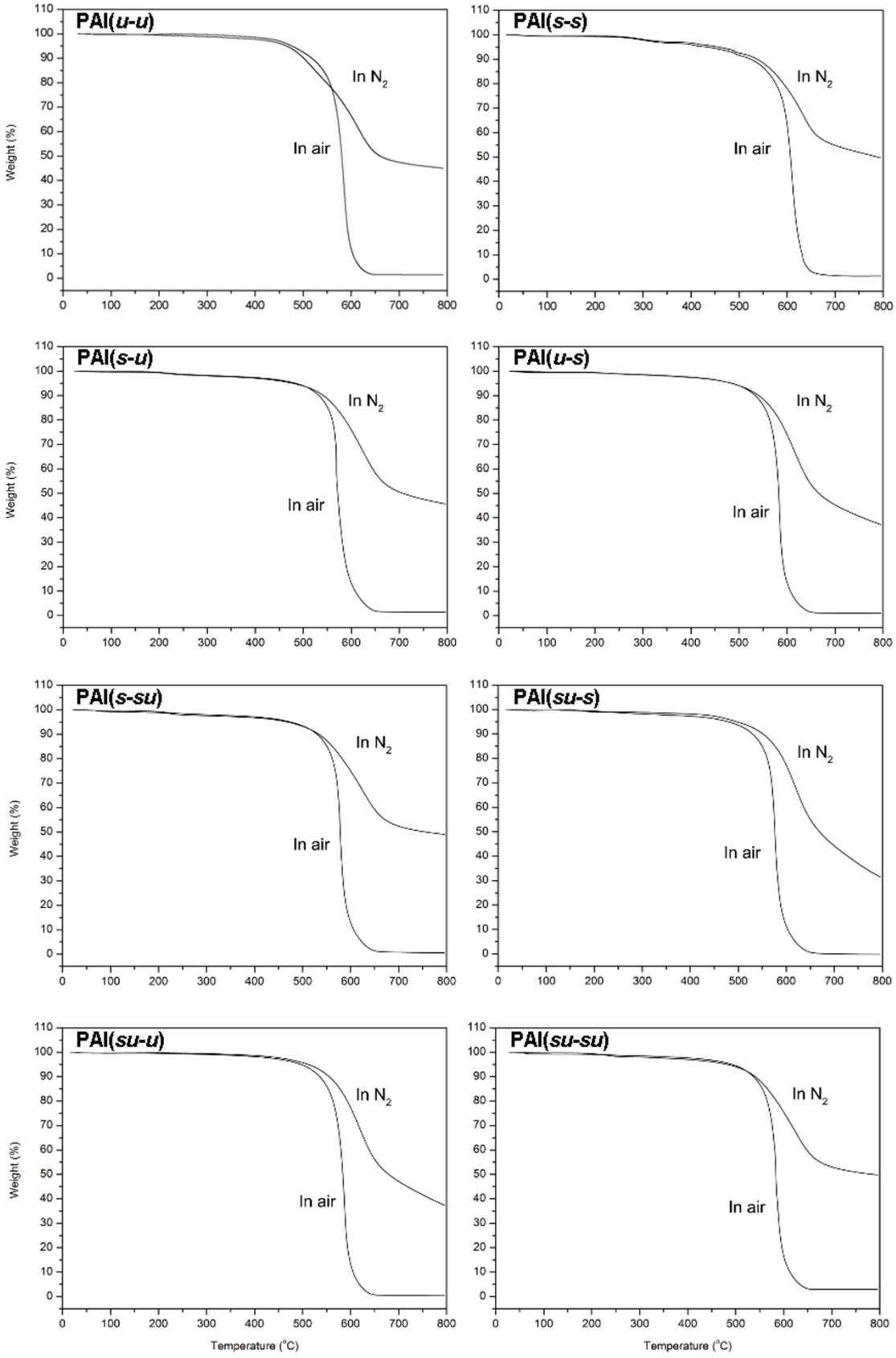

Fig. S12. TGA data of PAIs.

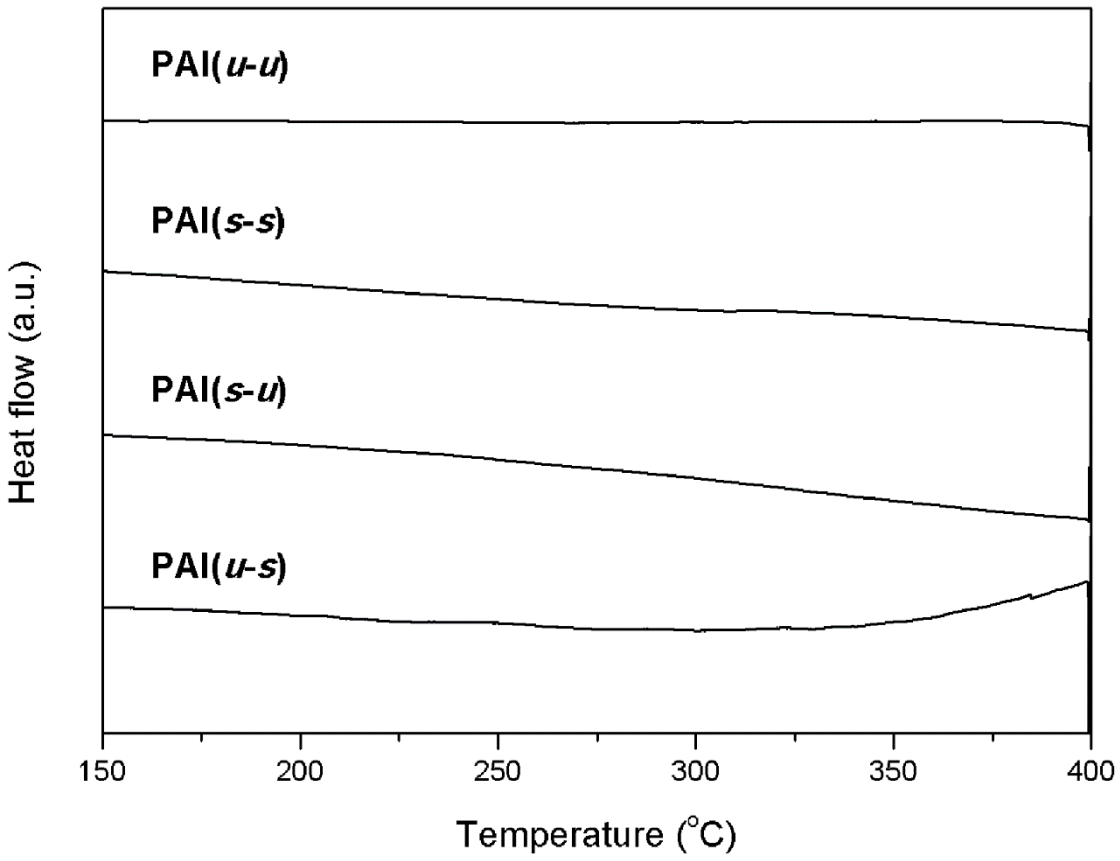

Fig. S13. DSC data of representative PAIs.

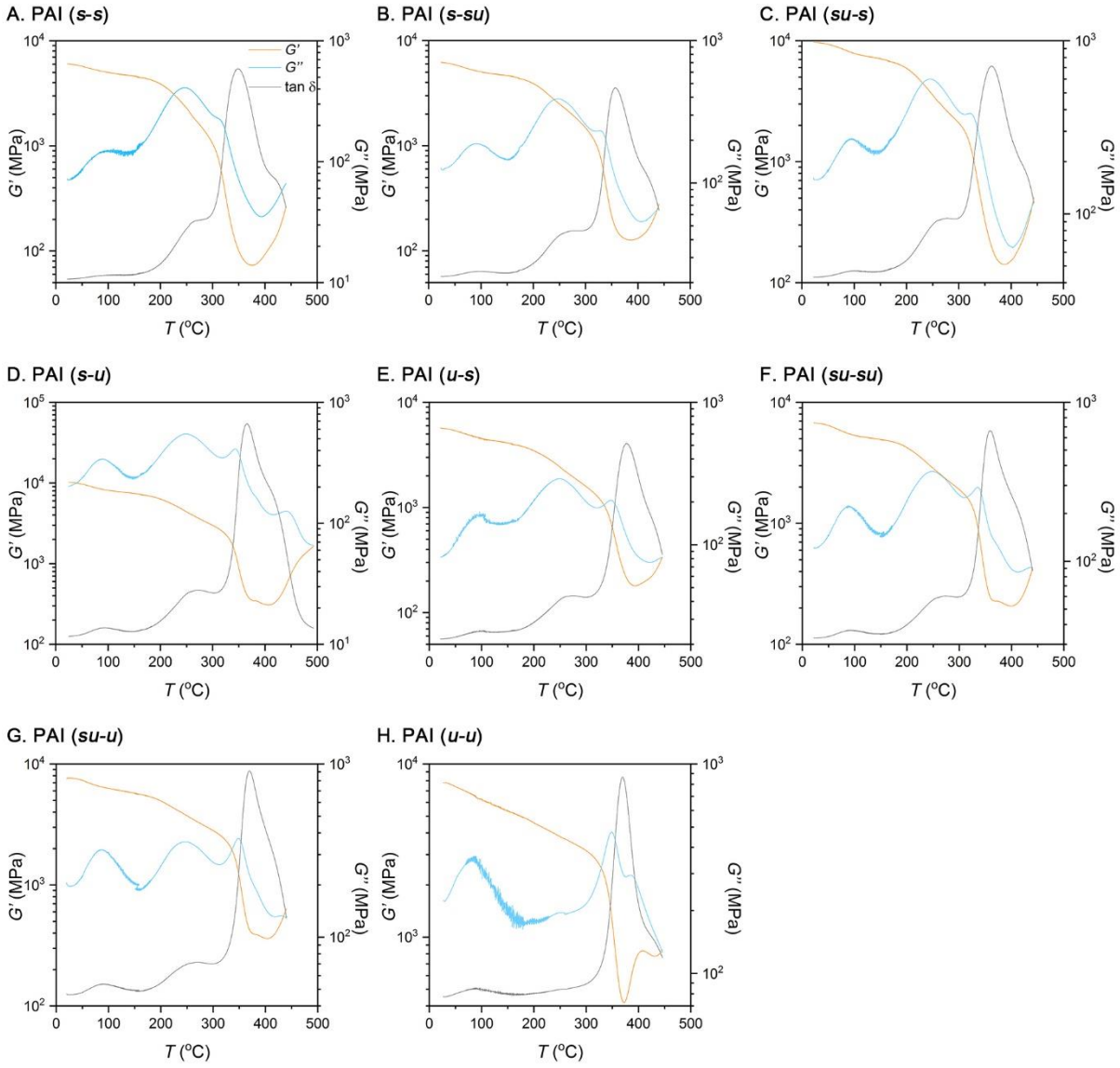

Fig. S14. DMA data of PAIs.

Table S3. Transition temperatures of PAIs identified by the DMA.

Entry	T_α (°C)	T_β (°C)	T_γ (°C)
PAI (*s-s*)	348.3	262.5	101.3
PAI (*s-su*)	357.3	257.9	93.1
PAI (*su-s*)	362.3	262	98.1
PAI (*s-u*)	365.8	266.4	92.4
PAI (*u-s*)	377.8	265.6	97.7
PAI (*su-su*)	359.2	261.6	88.6
PAI (*su-u*)	362.3	258.3	84.7
PAI (*u-u*)	369.1	-	89

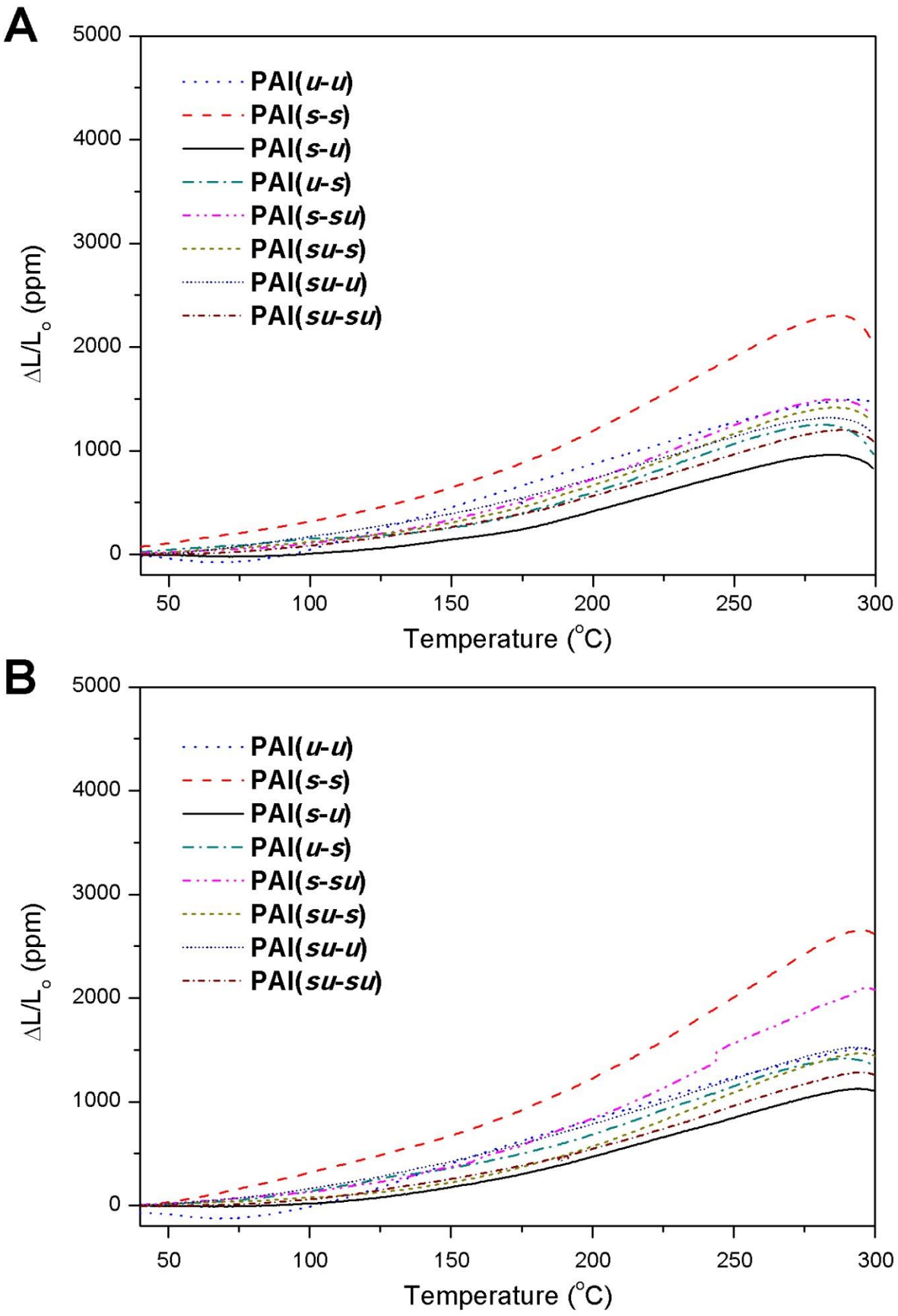

Fig. S15. TMA data of PAIs. (**A**) Second scans. (**B**) Third scans.

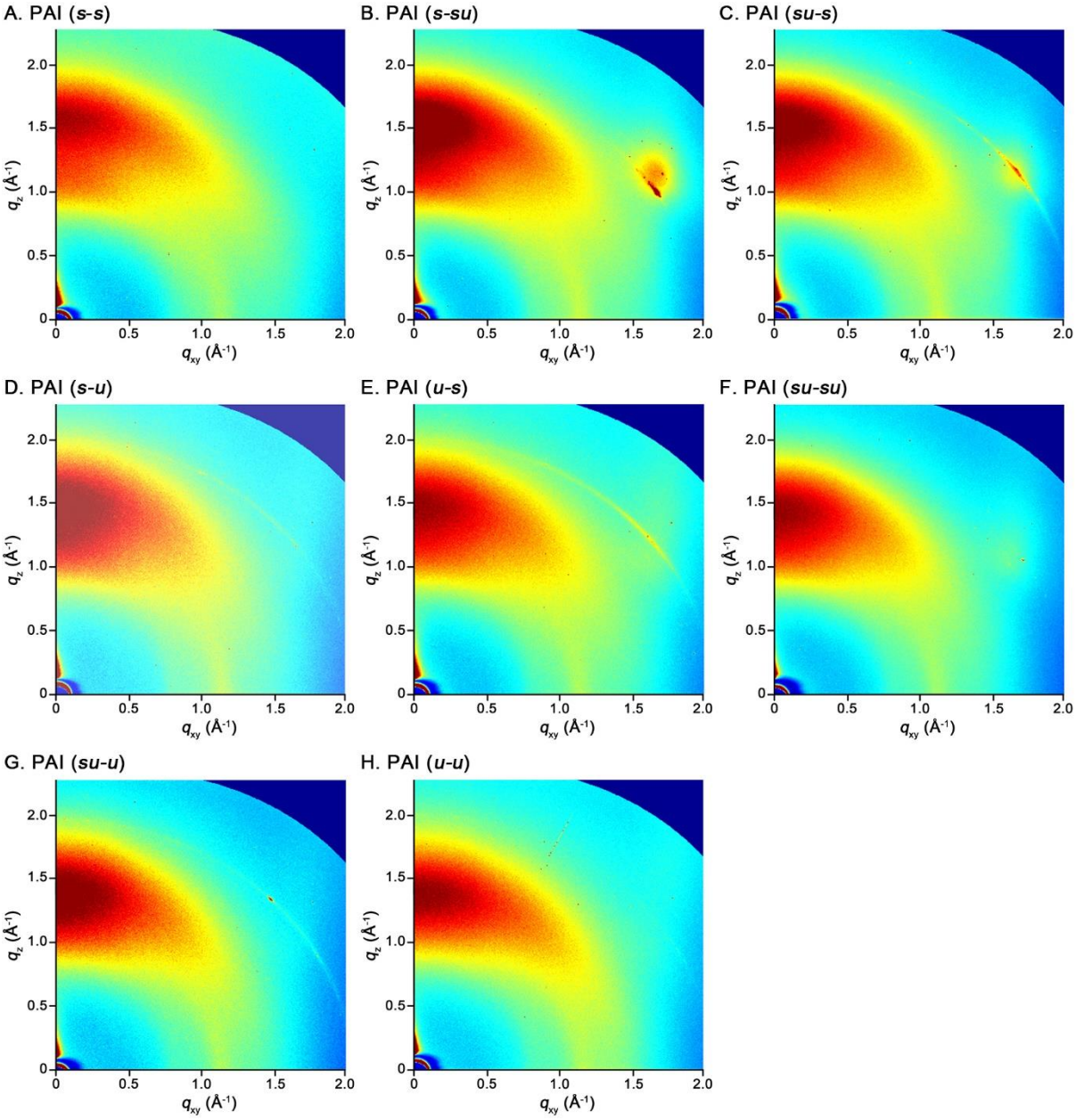

Fig. S16. 2D GIWAXS data of PAIs.

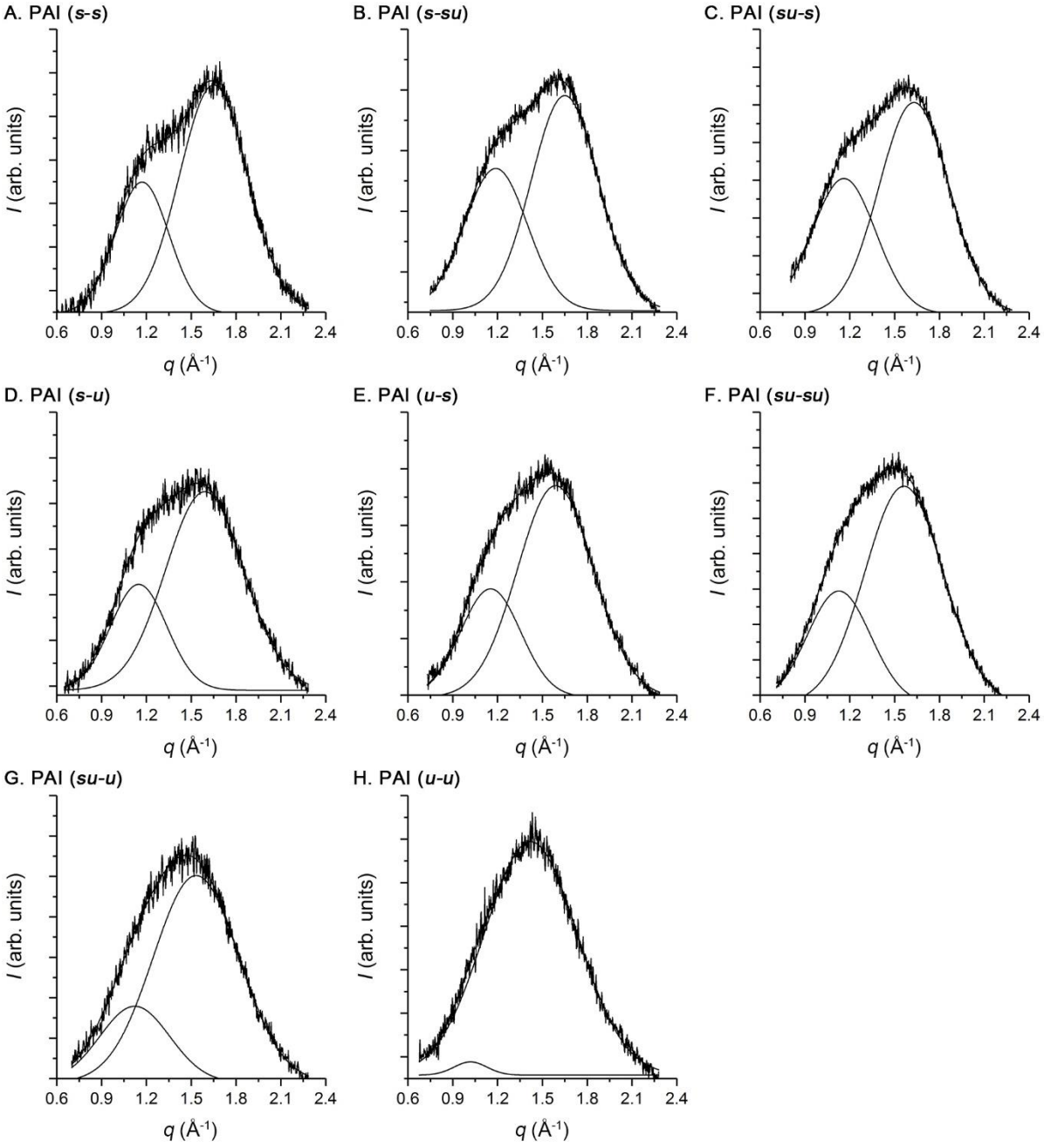

Fig. S17. 1D deconvoluted plot of the GIWAXS data in out-of-plane direction.

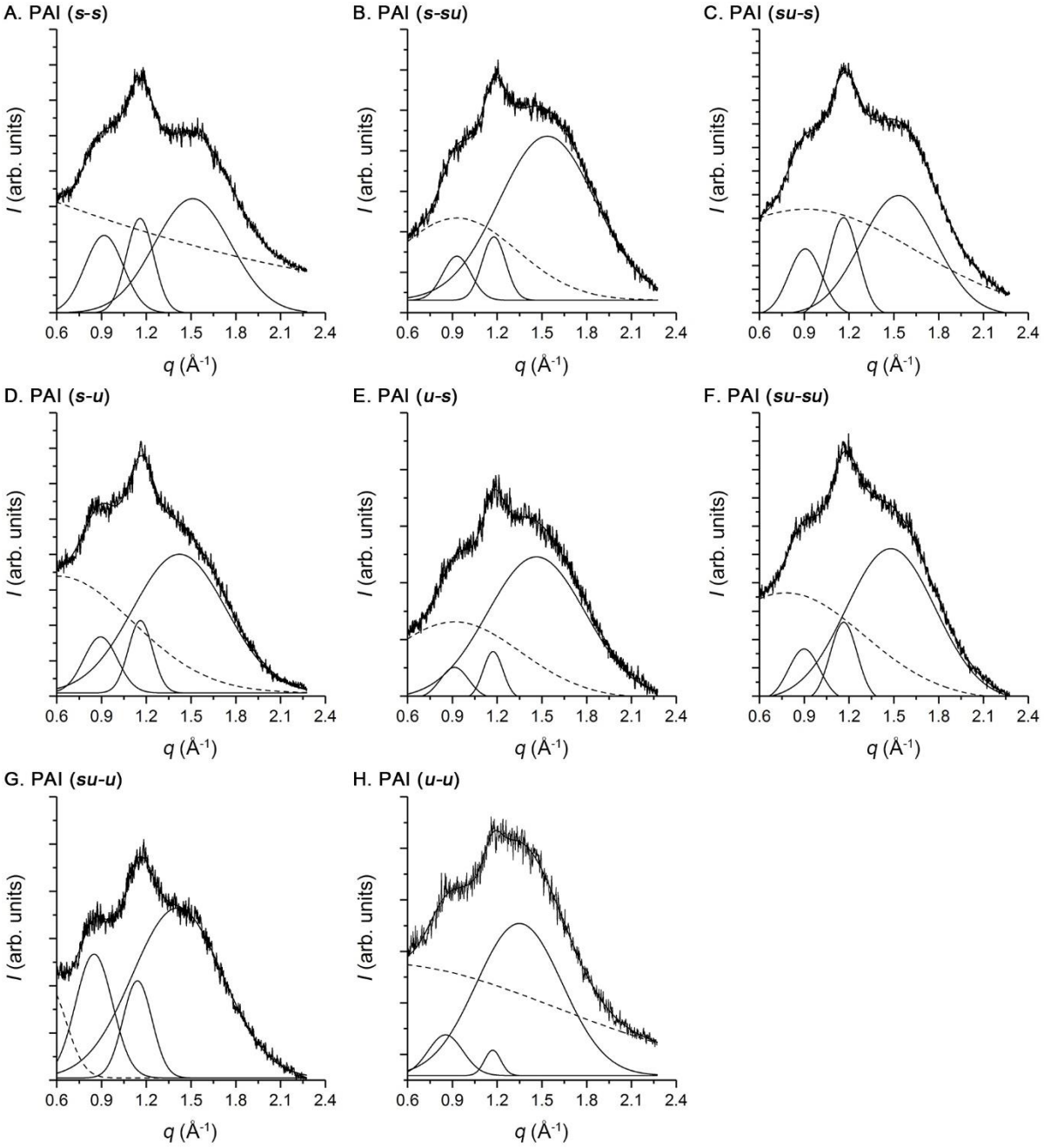

Fig. S18. 1D deconvoluted plot of the GIWAXS data in in-plane direction.

Table S4. Summary of the GIWAXS peak positions.

In-plane	Peak position ($Å^{-1}$)	Characteristic distance (Å)	Assign-ment	Out-of-plane	Peak position ($Å^{-1}$)	Characteristic distance (Å)	Assign-ment
PAI (*s*-*s*)	1.509	4.164		**PAI (*s*-*s*)**	1.650	3.808	π -π stack[b]
	1.158	5.426	ch-pack[a]		1.171	5.366	ch-pack
	0.918	6.844					
PAI (*s*-*su*)	1.536	4.091		**PAI (*s*-*su*)**	1.650	3.808	π -π stack
	1.178	5.334	ch-pack		1.188	5.289	ch-pack
	0.930	6.756					
PAI (*su*-*s*)	1.532	4.101		**PAI (*su*-*s*)**	1.630	3.855	π -π stack
	1.163	5.402	ch-pack		1.160	5.416	ch-pack
	0.907	6.927					
PAI (*s*-*u*)	1.422	4.418		**PAI (*s*-*u*)**	1.591	3.949	π -π stack
	1.161	5.412	ch-pack		1.148	5.473	ch-pack
	0.894	7.028					
PAI (*u*-*s*)	1.463	4.295		**PAI (*u*-*s*)**	1.588	3.957	π -π stack
	1.173	5.356	ch-pack		1.153	5.449	ch-pack
	0.914	6.874					
PAI (*su*-*su*)	1.480	4.245		**PAI (*su*-*su*)**	1.562	4.022	π -π stack
	1.164	5.398	ch-pack		1.127	5.575	ch-pack
	0.899	6.989					
PAI (*su*-*u*)	1.409	4.459		**PAI (*su*-*u*)**	1.533	4.099	π -π stack
	1.141	5.507	ch-pack		1.122	5.600	ch-pack
	0.850	7.392					
PAI (*u*-*u*)	1.349	4.658		**PAI (*u*-*u*)**	1.422	4.418	π -π stack
	1.170	5.370	ch-pack		1.019	6.166	ch-pack
	0.854	7.357					

[a]ch-pack: the interchain packing distance of polymer chains. [b]π -π stack: face-to-face π-stacking distance of polymer chains.

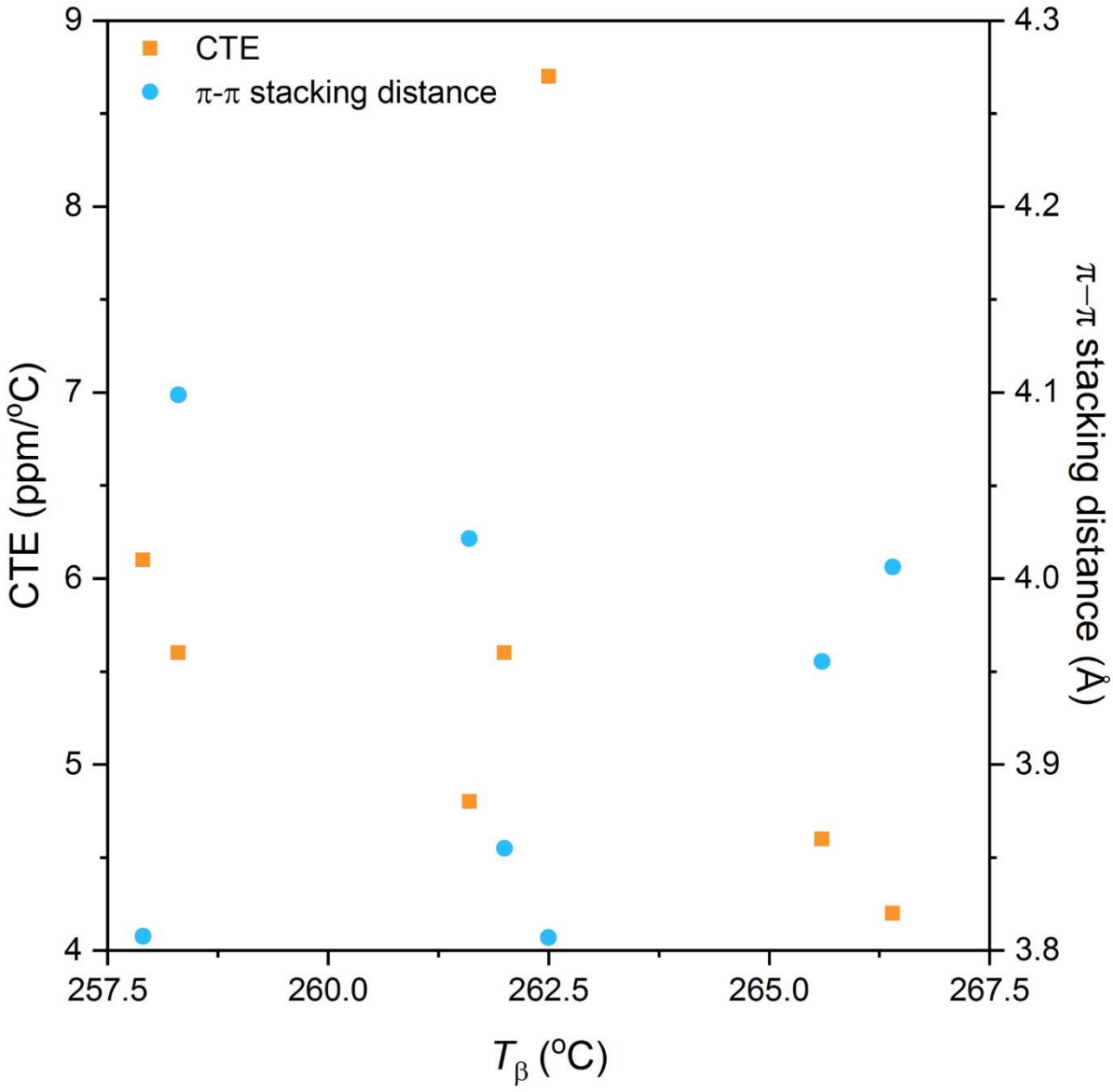

Fig. S19. A plot of CTE and π-π stacking distance versus β-relaxation temperature determined by the DMA.

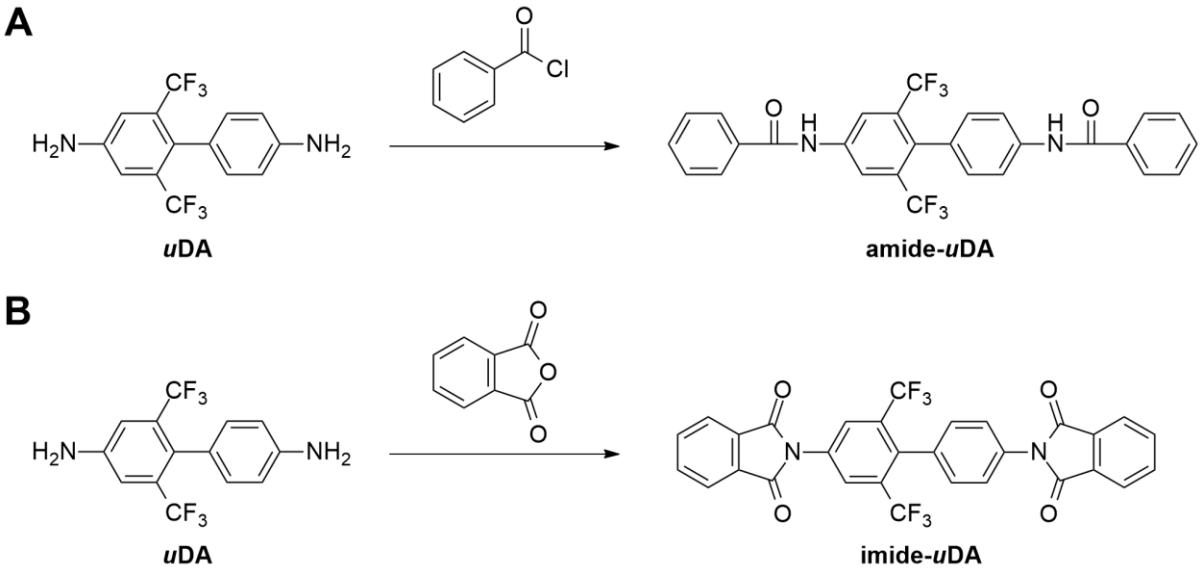

Fig. S20. Synthetic route to model compound (A) amide-*u*DA and (B) imide-*u*DA.

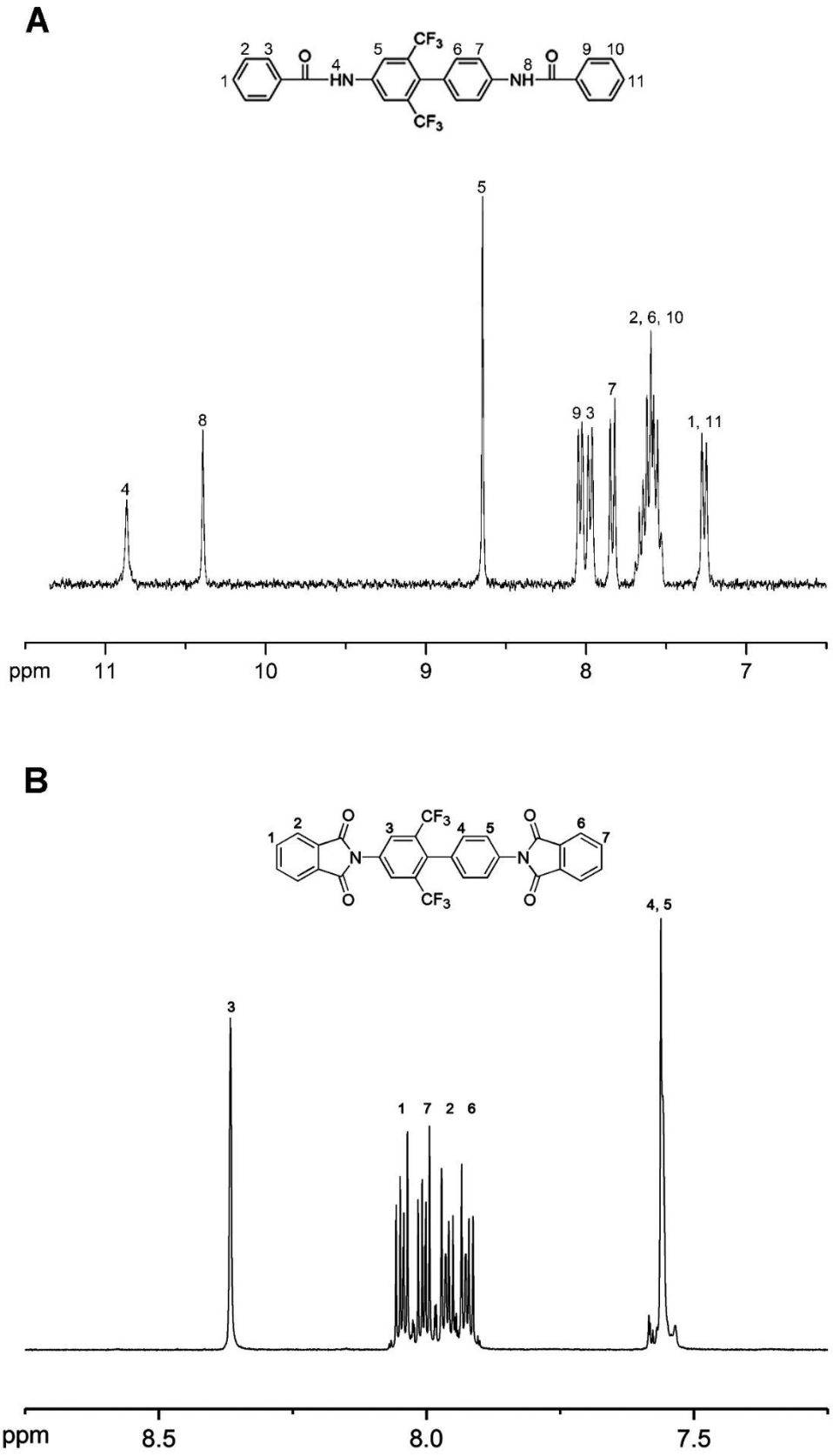

Fig. S21. ^{1}H NMR spectra of model compound (A) amide-*u*DA and (B) imide-*u*DA.

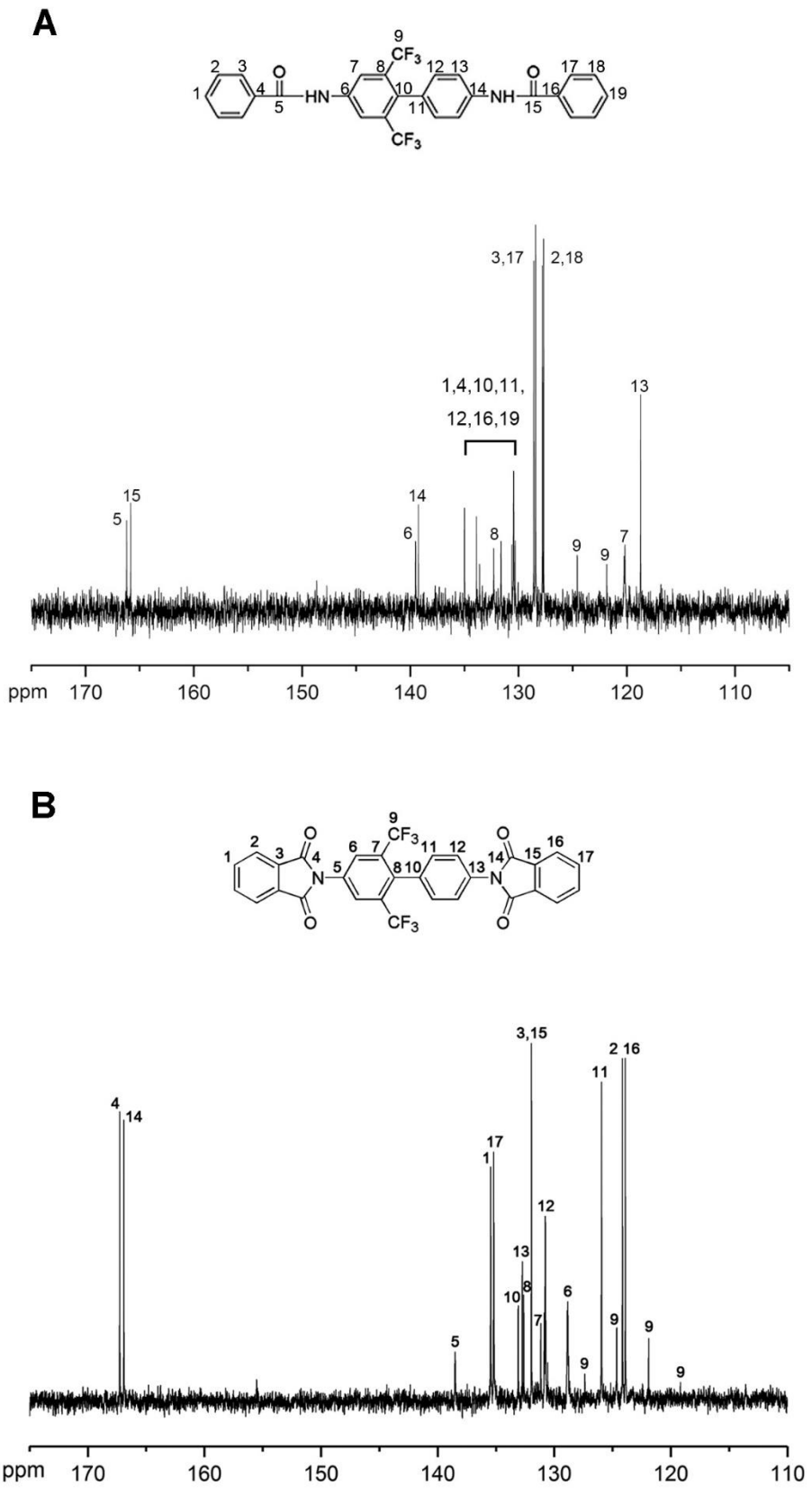

Fig. S22. ^{13}C NMR spectra of model compound (A) amide-*u*DA and (B) imide-*u*DA.

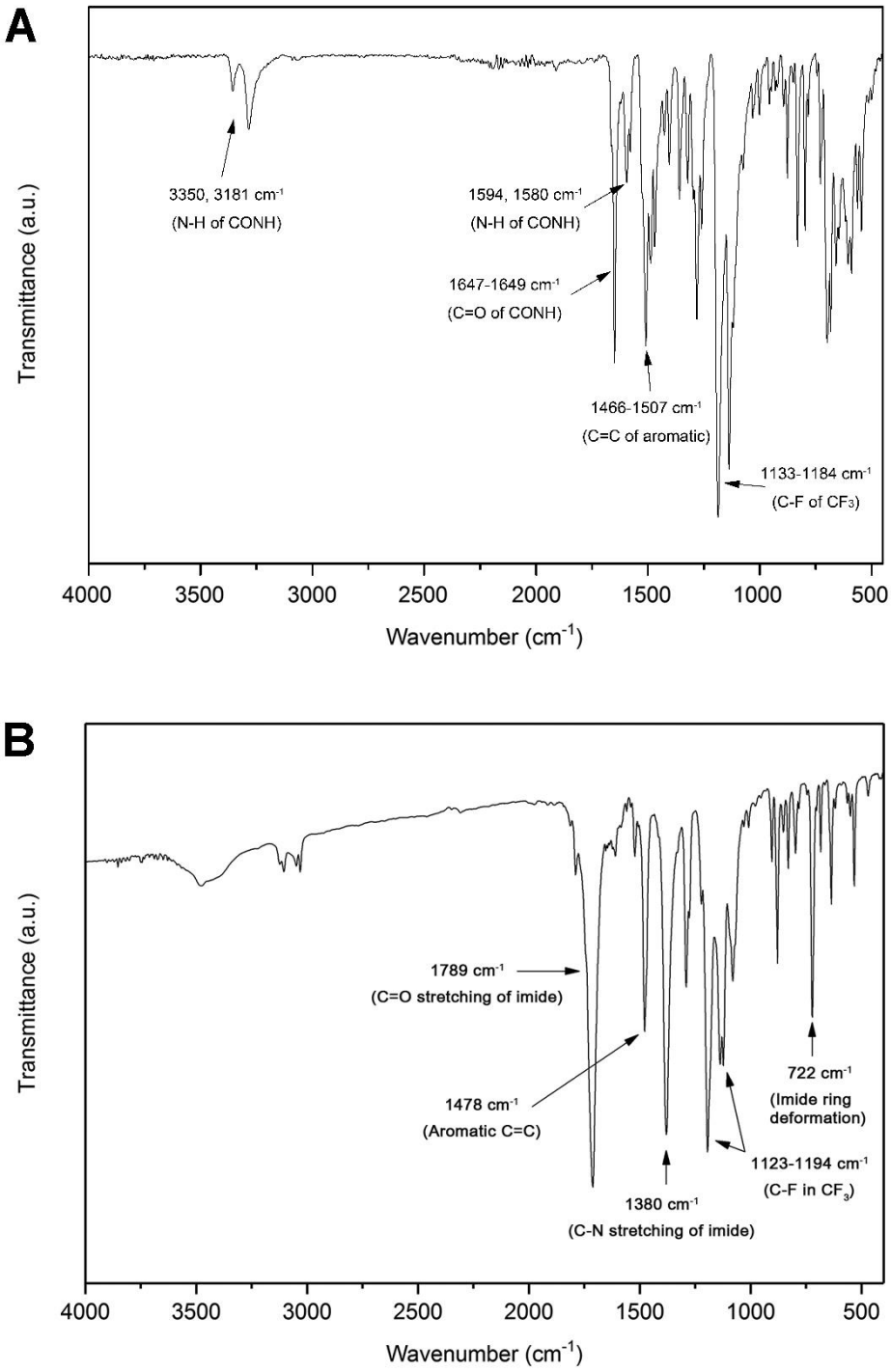

Fig. S23. FTIR spectra of model compound (A) amide-*u*DA and (B) imide-*u*DA.

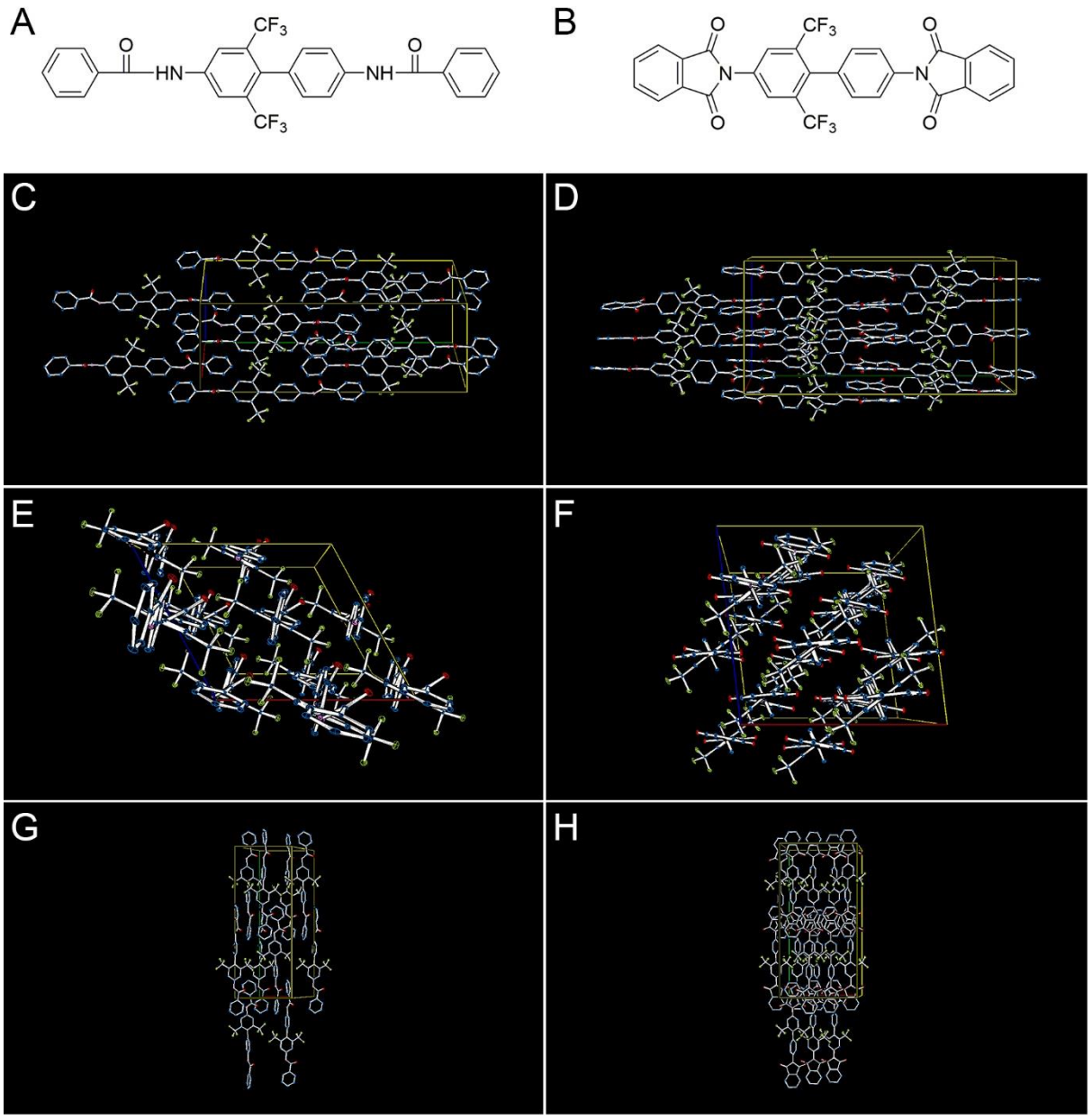

Fig. S24. (A, B) Chemical structure of amide-*u*DA (A) and imide-*u*DA (B) model compounds. (**C**, **E**, **G**) Crystal structure of **amide-*u*DA** in (100), (010), and (001) directions. (**D**, **F**, **H**) Crystal structure of **imide-*u*DA** in (100), (010), and (001) directions. Full crystallographic details can be obtained free of charge from the Cambridge Crystallographic Data Center via www.ccdc.cam.ac.uk/data_request/cif (CCDC 1587696 and 1587708).

Tables S5. Crystal data and structure refinement for amide-*u*DA.

Empirical formula	C28 H16 F6 N2 O2
Formula weight	528.44
Temperature	120(2) K
Wavelength	0.71073 Å
Crystal system	Monoclinic
Space group	C c
Unit cell dimensions	a = 10.3506(18) Å
b = 27.652(5) Å	
c = 9.1626(16) Å	
Volume	2300.7(7) $Å^3$
Z	4
Density (calculated)	1.526 Mg/m^3
Absorption coefficient	0.130 mm^{-1}
F(000)	1080.0
Crystal size	0.380 x 0.140 x 0.120 mm^3
Theta range for data collection	2.361 to 26.472°.
Index ranges	-12<=h<=12, -34<=k<=34, -11<=l<=11
Reflections collected	30188
Independent reflections	4724 [R(int) = 0.1092]
Completeness to theta = 25.242°	100.0 %
Refinement method	Full-matrix least-squares on F^2
Data / restraints / parameters	4724 / 2 / 343
Goodness-of-fit on F^2	1.034
Final R indices [I>2sigma(I)]	R1 = 0.0920, wR2 = 0.2179
R indices (all data)	R1 = 0.1361, wR2 = 0.2519
Extinction coefficient	n/a
Largest diff. peak and hole	0.589 and -0.525 $e.Å^{-3}$

Tables S6. Crystal data and structure refinement for imide-*u*DA.

Empirical formula	C30 H14 F6 N2 O4
Formula weight	580.43
Temperature	120(2) K
Wavelength	0.71073 Å
Crystal system	Monoclinic
Space group	C 2/c
Unit cell dimensions	a = 13.8533(10) Å
	b = 27.477(2) Å
	c = 13.4481(10) Å
Volume	5082.3(7) $Å^3$
Z	8
Density (calculated)	1.517 Mg/m^3
Absorption coefficient	0.131 mm^{-1}
F(000)	2352
Crystal size	0.200 x 0.100 x 0.050 mm^3
Theta range for data collection	1.656 to 27.760°.
Index ranges	-17<=h<=18, -35<=k<=35, -16<=l<=17
Reflections collected	46515
Independent reflections	5824 [R(int) = 0.1092]
Completeness to theta = 25.242°	99.9 %
Refinement method	Full-matrix least-squares on F^2
Data / restraints / parameters	5824 / 0 / 379
Goodness-of-fit on F^2	1.027
Final R indices [I>2sigma(I)]	R1 = 0.0921, wR2 = 0.2408
R indices (all data)	R1 = 0.1674, wR2 = 0.3036
Extinction coefficient	n/a
Largest diff. peak and hole	1.152 and -0.443 $e.Å^{-3}$

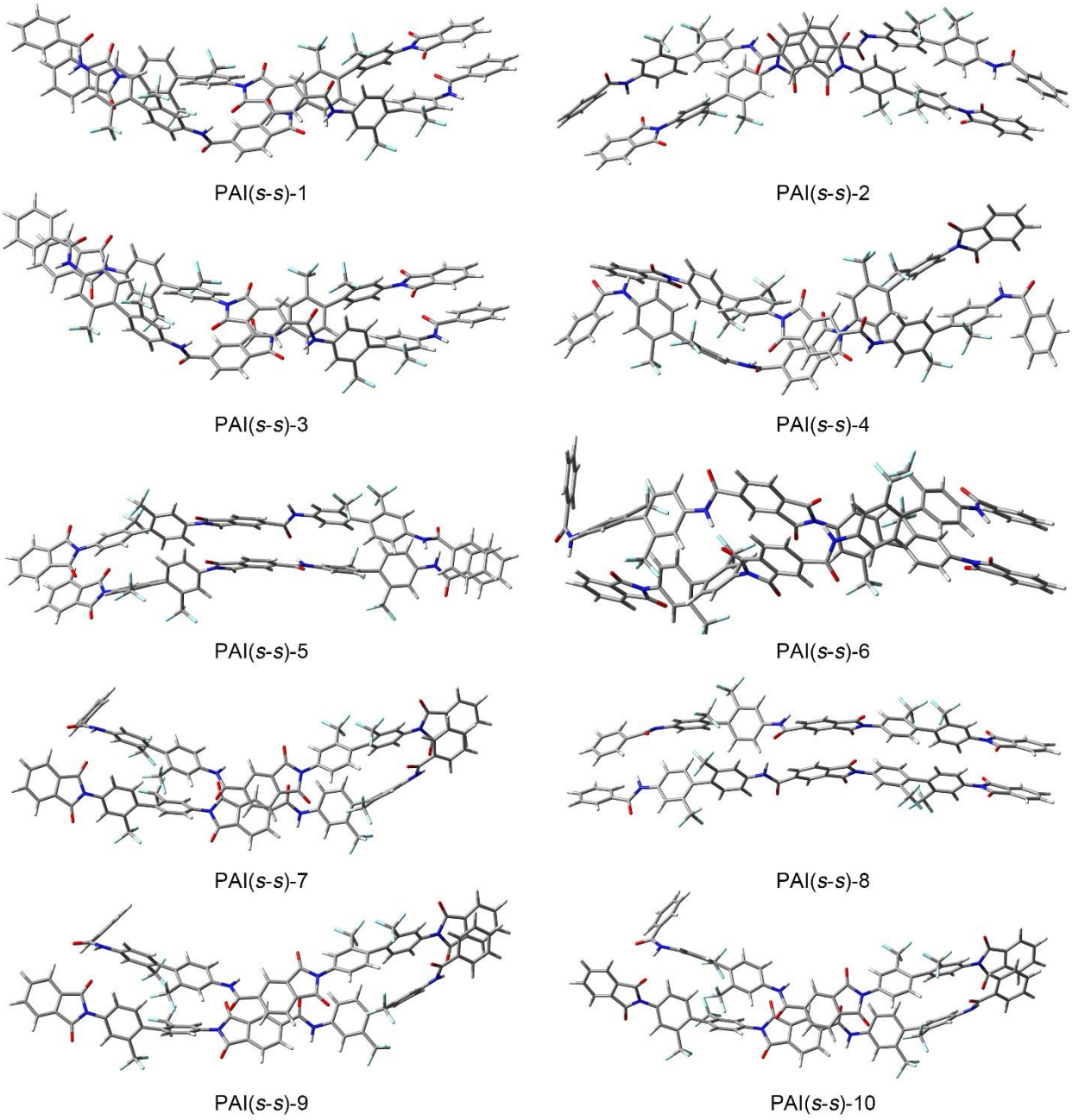

Fig. S25. Ten most stable structures of PAI(*s*-*s*).

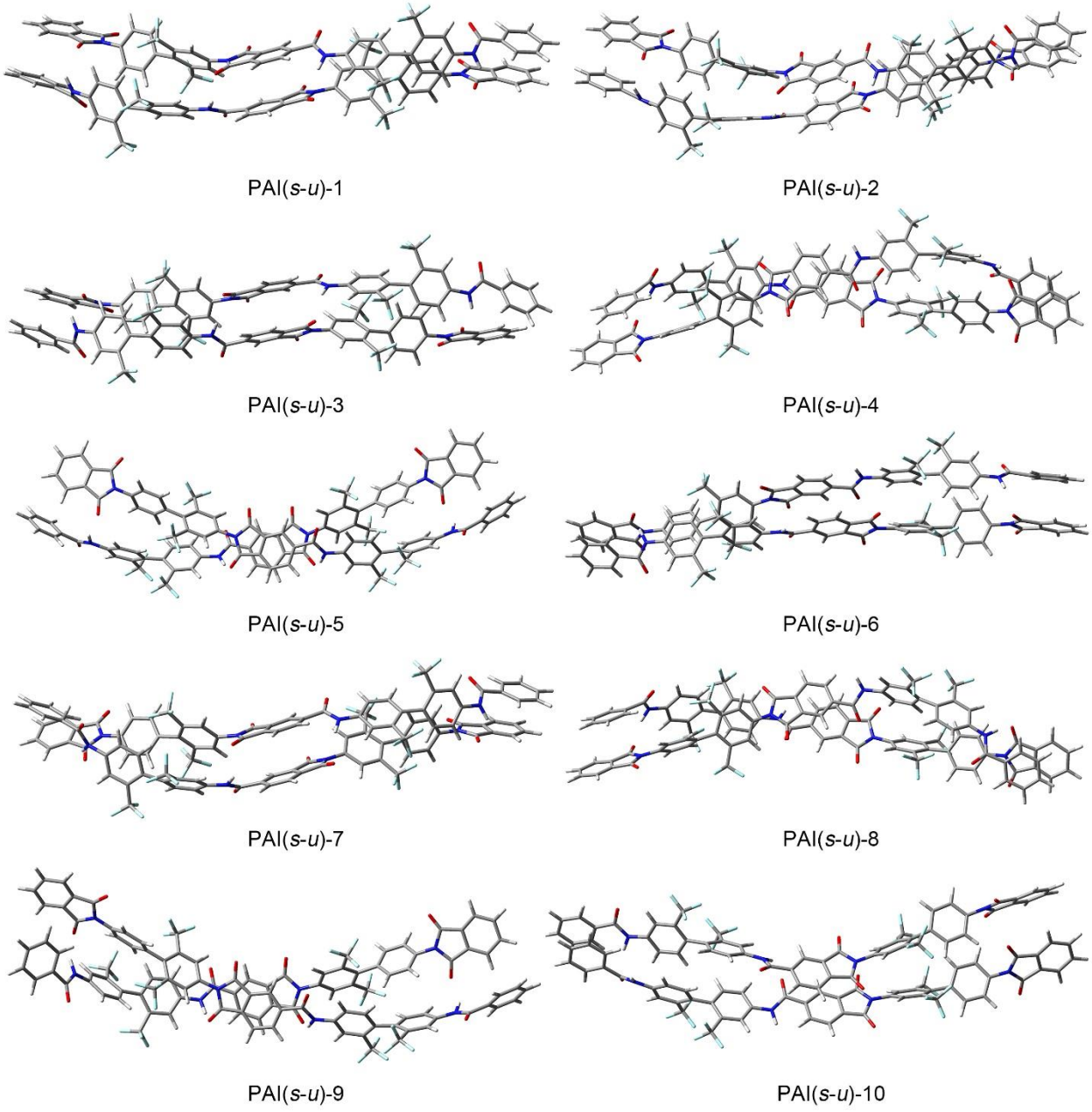

Fig. S26. Ten most stable structures of PAI(*s*-*u*).

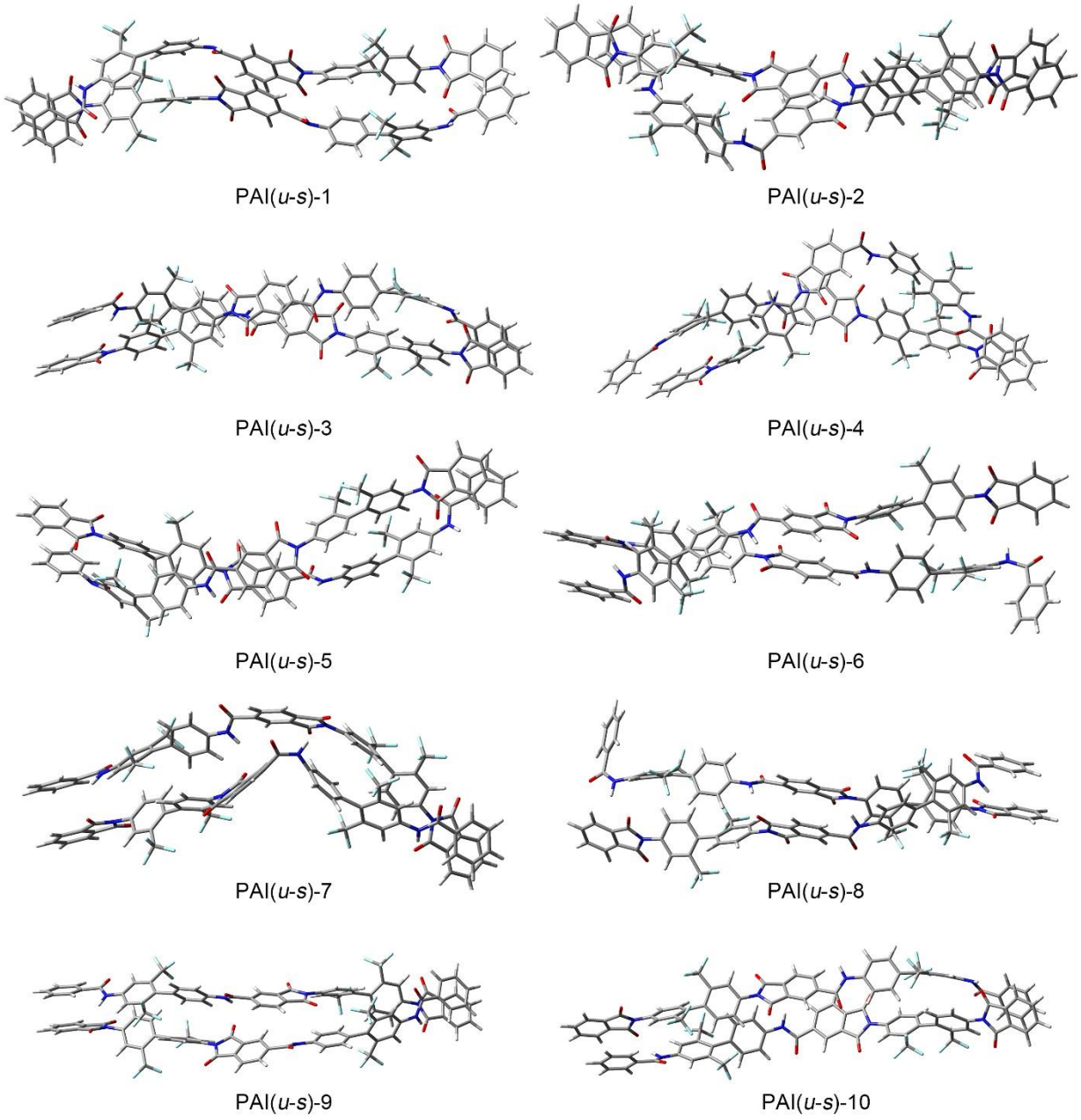

Fig. S27. Ten most stable structures of PAI(*u*-*s*).

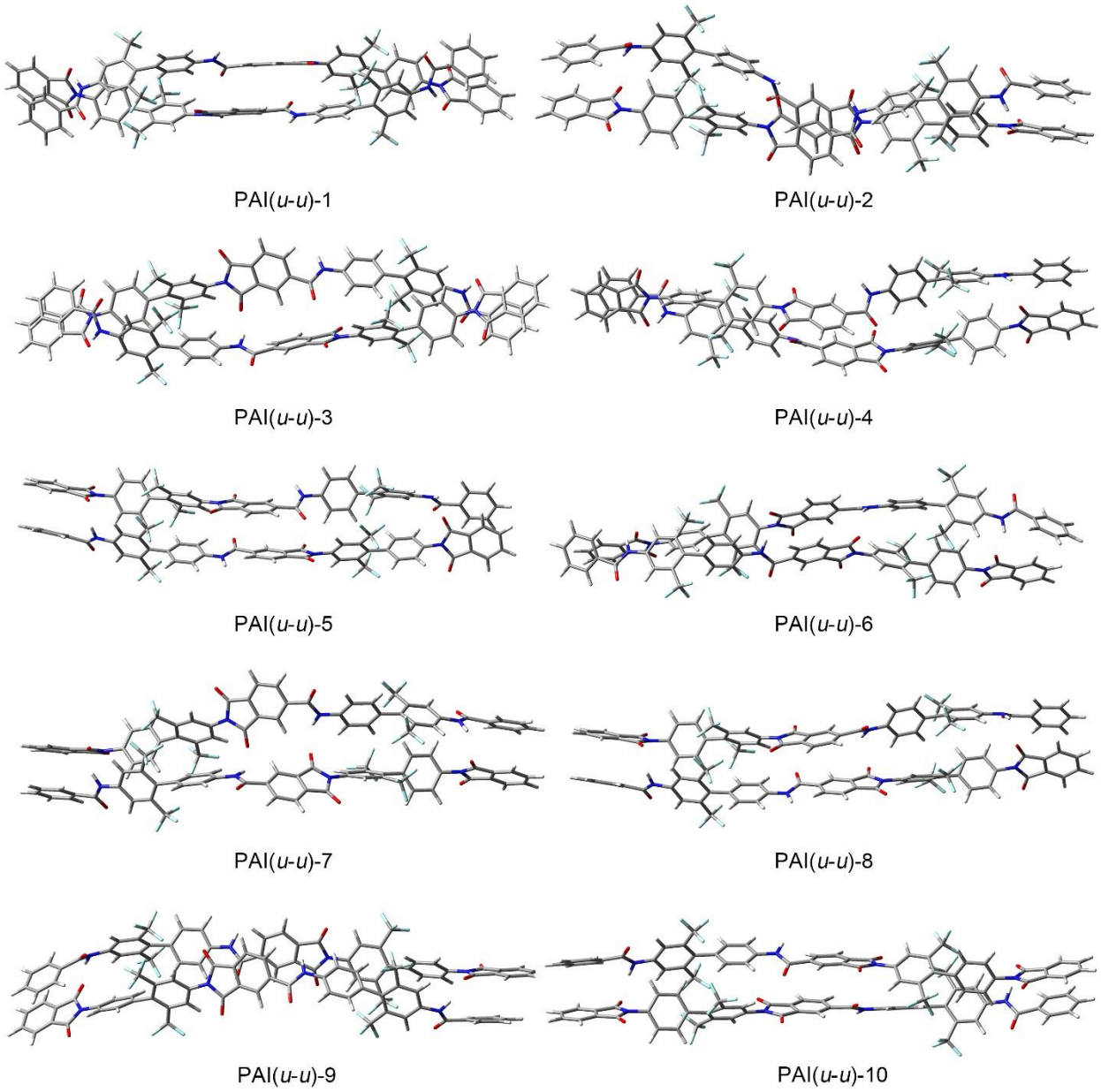

Fig. S28. Ten most stable structures of PAI(*u*-*u*).

Table S7. Bonding energies and geometric features of the 10 most stable dimeric structures for each of PAI(*s*-*s*), PAI(*s*-*u*), PAI(*u*-*s*), and PAI(*u*-*u*).

Name	Bonding Energy (kcal/mol)	Parallel(P)/ Anti-parallel(A)	Inter-twined?	Name	Bonding Energy (kcal/mol)	Parallel(P)/ Anti-parallel(A)	Inter-twined?
PAI(*s*-*s*)-1	-67.8	A	Yes	**PAI(*u*-*s*)-1**	-68.1	A	Yes
PAI(*s*-*s*)-2	-66.3	A	Yes	**PAI(*u*-*s*)-2**	-65.4	A	No
PAI(*s*-*s*)-3	-66.2	A	Yes	**PAI(*u*-*s*)-3**	-65.5	A	Yes
PAI(*s*-*s*)-4	-62.6	A	Yes	**PAI(*u*-*s*)-4**	-63.3	A	Yes
PAI(*s*-*s*)-5	-62.5	P	No	**PAI(*u*-*s*)-5**	-62.2	A	Yes
PAI(*s*-*s*)-6	-59.7	A	Yes	**PAI(*u*-*s*)-6**	-61.4	A	Yes
PAI(*s*-*s*)-7	-54.6	A	No	**PAI(*u*-*s*)-7**	-61.4	A	No
PAI(*s*-*s*)-8	-53.5	P	No	**PAI(*u*-*s*)-8**	-61.0	A	Yes
PAI(*s*-*s*)-9	-52.9	A	No	**PAI(*u*-*s*)-9**	-60.9	A	No
PAI(*s*-*s*)-10	-52.4	A	No	**PAI(*u*-*s*)-10**	-60.5	A	No
PAI(*s*-*u*)-1	-65.2	A	No	**PAI(*u*-*u*)-1**	-61.6	A	Yes
PAI(*s*-*u*)-2	-65.1	A	No	**PAI(*u*-*u*)-2**	-60.1	A	No
PAI(*s*-*u*)-3	-63.4	A	No	**PAI(*u*-*u*)-3**	-59.1	A	Yes
PAI(*s*-*u*)-4	-64.9	A	Yes	**PAI(*u*-*u*)-4**	-59.0	A	No
PAI(*s*-*u*)-5	-61.8	A	Yes	**PAI(*u*-*u*)-5**	-58.6	A	No
PAI(*s*-*u*)-6	-62.8	A	No	**PAI(*u*-*u*)-6**	-55.8	A	No
PAI(*s*-*u*)-7	-61.5	A	Yes	**PAI(*u*-*u*)-7**	-56.0	A	Yes
PAI(*s*-*u*)-8	-62.0	A	Yes	**PAI(*u*-*u*)-8**	-56.6	A	No
PAI(*s*-*u*)-9	-59.8	A	Yes	**PAI(*u*-*u*)-9**	-56.3	A	No
PAI(*s*-*u*)-10	-60.1	P	No	**PAI(*u*-*u*)-10**	-56.0	A	No

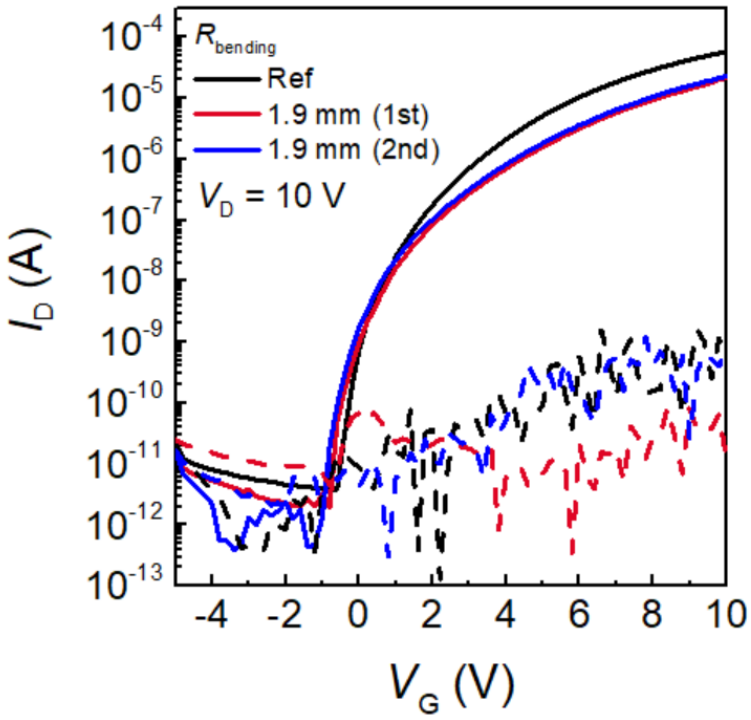

Fig. S29. Transfer characteristics of the IGZO TFTs under study. Black curve refers to the characteristics measured before bending; red one refers to the characteristics measured flat after being bent 10 times at a bending radius of 1.9mm; blue one indicates the characteristics measured flat one hour after the first run of the bending experiment.